

Estimating magnetic helicity in the Sun

Kostas Moraitis

LESIA, Observatoire de Paris, PSL Research University, CNRS, Sorbonne Universités,
UPMC Univ. Paris 06, Univ. Paris Diderot, Sorbonne Paris Cité,
5 place Jules Janssen, 92195 Meudon, France

in collaboration with

M.K. Georgoulis, K. Tziotziou (RCAAM of the Academy of Athens)
V. Archontis (St Andrews University), A. Nindos (University of Ioannina), ...



Outline

- Introduction – Magnetic helicity, Free energy
- Validation of a connectivity-based method for helicity computation
- Free energy vs helicity diagram
- Comparison of methods for the estimation of magnetic helicity
 - A Sun-to-Earth analysis of a solar eruption
 - In finite volumes
- Concluding remarks

Introduction

Magnetic helicity – Free magnetic energy

Magnetic helicity

- Measure of twist and distortion of mfl
- Topological invariant
- Gauss linking number
- Signed quantity (+ right handed, - left handed)
- Splits into self + mutual terms
- Helicity represents the amount of flux linkages between pairs of lines
- Approximately conserved in reconnection
- Emerges via helical magnetic flux tubes and/or is generated by photospheric proper motions
- An isolated configuration with accumulated magnetic helicity cannot relax to a potential field
- If not transferred to larger scales it can only be expelled bodily in the form of CMEs

$$H = \int \mathbf{A} \cdot \mathbf{B} dV \quad \mathbf{B} = \nabla \times \mathbf{A}$$

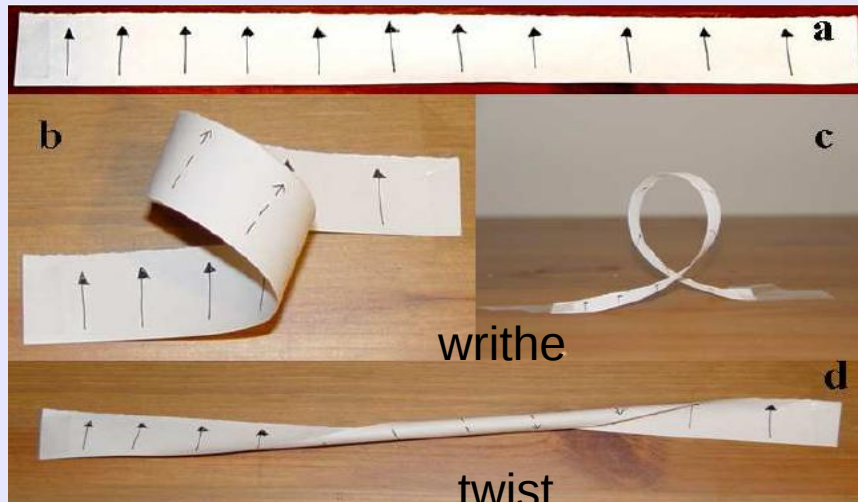
Free magnetic energy

- Excess energy above potential state
- Energy available for solar flares + CMEs

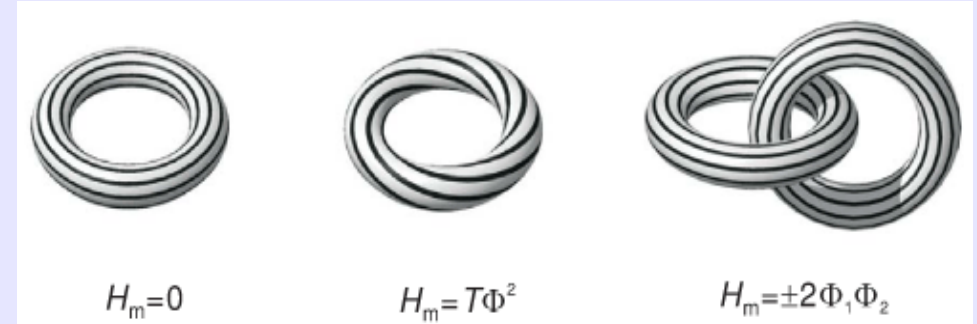
$$E_c = \frac{1}{8\pi} \int dV \mathbf{B}^2 - \frac{1}{8\pi} \int dV \mathbf{B}_p^2$$

Introduction Relative magnetic helicity

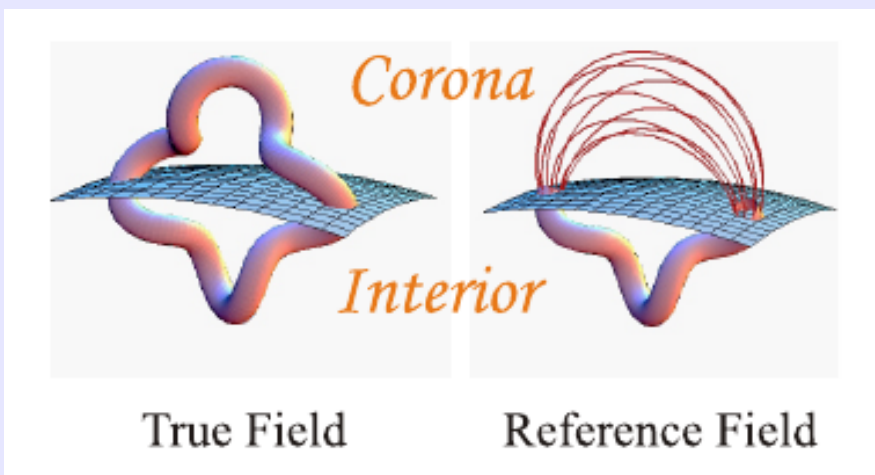
single flux tube



two closed flux tubes



$$H = (Tw + Wr)\Phi^2$$



$$H = \int \mathbf{A} \cdot \mathbf{B} dV$$

gauge invariant for closed + solenoidal \mathbf{B}

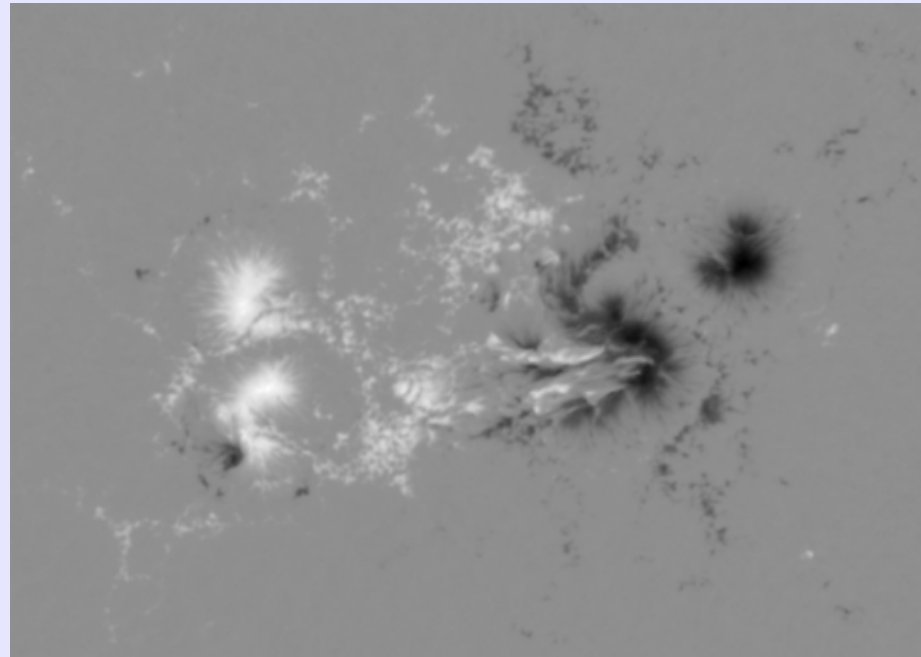
$$H = \int (\mathbf{A} + \mathbf{A}_p) \cdot (\mathbf{B} - \mathbf{B}_p) dV$$

gauge invariant for closed + solenoidal $\mathbf{B} - \mathbf{B}_p$

Connectivity method

Steps:

1. partition vector magnetogram into flux concentrations
2. create connectivity matrix with flux committed to opposite polarity partitions (simulated annealing method)
3. each connection=flux tube with known flux Φ , FF parameter α , position

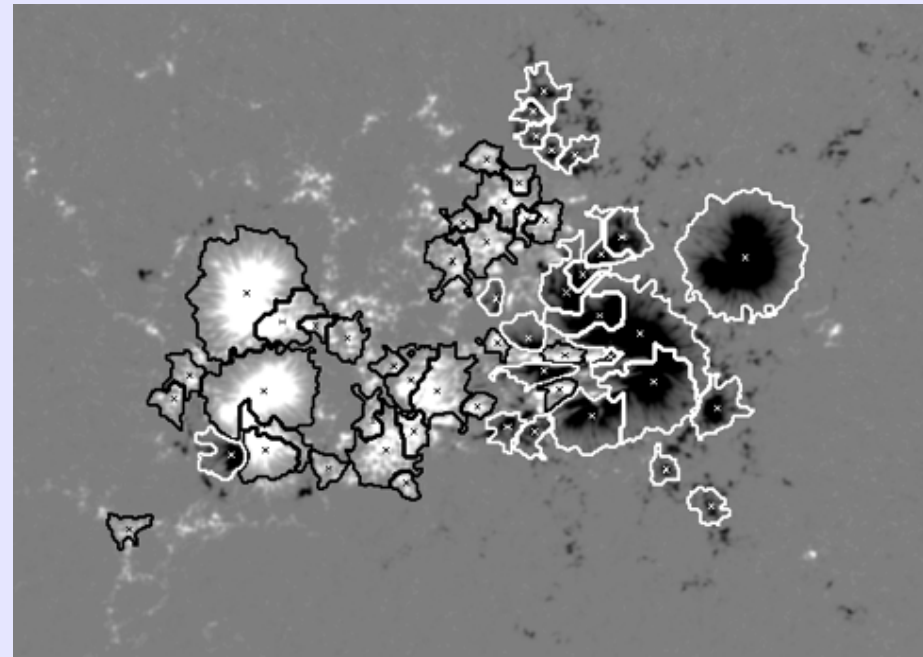


Georgoulis & LaBonte 2007, Georgoulis+ 2012

Connectivity method

Steps:

1. partition vector magnetogram into flux concentrations
2. create connectivity matrix with flux committed to opposite polarity partitions (simulated annealing method)
3. each connection=flux tube with known flux Φ , FF parameter α , position

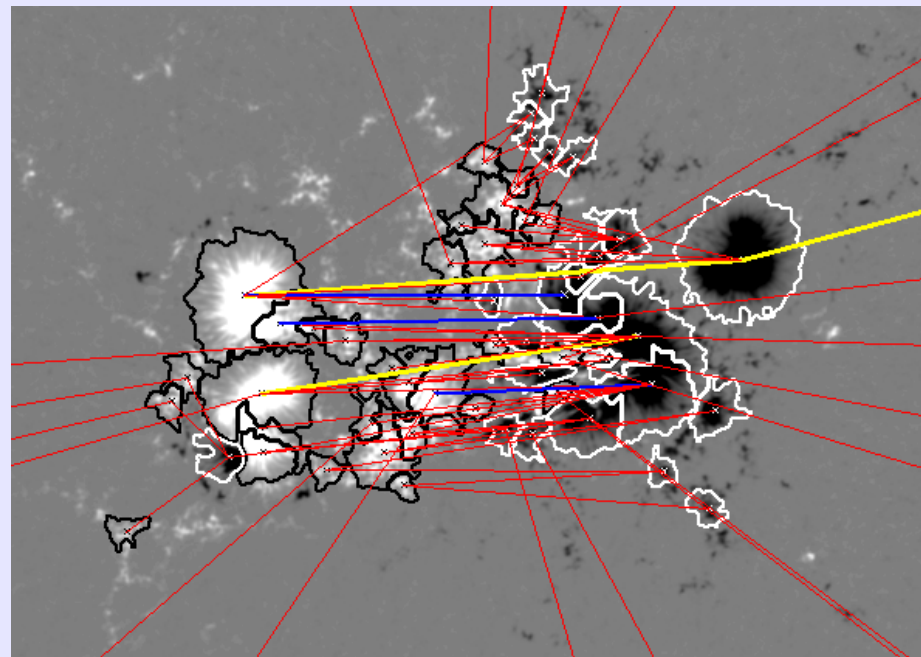


Georgoulis & LaBonte 2007, Georgoulis+ 2012

Connectivity method

Steps:

1. partition vector magnetogram into flux concentrations
2. create connectivity matrix with flux committed to opposite polarity partitions (simulated annealing method)
3. each connection=flux tube with known flux Φ , FF parameter α , position



Georgoulis & LaBonte 2007, Georgoulis+ 2012

Connectivity method

Steps:

1. partition vector magnetogram into flux concentrations
2. create connectivity matrix with flux committed to opposite polarity partitions (simulated annealing method)
3. each connection=flux tube with known flux Φ , FF parameter α , position

$$H = 8\pi d^2 A \sum_{l=1}^N \alpha_l \Phi_l^{2\lambda} + \sum_{l=1}^N \sum_{m=1, l \neq m}^N \mathcal{L}_{lm}^{arch} \Phi_l \Phi_m$$

| self terms | mutual terms |
|--|--------------|
| $E_c = Ad^2 \sum_{l=1}^N \alpha_l^2 \Phi_l^{2\lambda} + \frac{1}{8\pi} \sum_{l=1}^N \sum_{m=1, l \neq m}^N \alpha_l \mathcal{L}_{lm}^{arch} \Phi_l \Phi_m$ | |

A, λ : constants, N : # of FTs, d : pixel size, \mathcal{L}^{arch} : arch number (Demoulin+ 2006)

Important note: E_c budget is a lower-limit

Georgoulis & LaBonte 2007, Georgoulis+ 2012

Volume method

| | | |
|----------------------------|--|--|
| Relative magnetic helicity | $H = \int dV (\mathbf{A} + \mathbf{A}_p) \cdot (\mathbf{B} - \mathbf{B}_p)$ | } |
| self helicity | $H_{self} = \int dV (\mathbf{A} - \mathbf{A}_p) \cdot (\mathbf{B} - \mathbf{B}_p)$ | |
| mutual (?) helicity | $H_{mut} = 2 \int dV \mathbf{A}_p \cdot (\mathbf{B} - \mathbf{B}_p)$ | |
| | | gauge invariant for closed + solenoidal $\mathbf{B}_c = \mathbf{B} - \mathbf{B}_p$ |
| Free magnetic energy | $E_{c1} = \frac{1}{8\pi} \int dV \mathbf{B}^2 - \frac{1}{8\pi} \int dV \mathbf{B}_p^2$ | } |
| | $E_{c2} = \frac{1}{8\pi} \int dV (\mathbf{B} - \mathbf{B}_p)^2$ | |
| | | equivalent for closed + solenoidal $\mathbf{B}_c = \mathbf{B} - \mathbf{B}_p$ |

The task is: for given 3D field \mathbf{B} compute \mathbf{B}_p , \mathbf{A} , \mathbf{A}_p

Volume method

step 1: Calculation of potential field $\mathbf{B}_p = -\nabla \varphi$

solve numerically Laplace's equation

$$\nabla^2 \varphi = 0$$

with Neumann BCs

$$(-\partial \varphi / \partial \hat{n})_{\partial V} = (\hat{n} \cdot \mathbf{B})_{\partial V}$$

- FISHPACK routine HW3CRT (similar to NAG routine D03FAF)
- BVP well defined only for flux-balanced 3D field
(check with 2 flags) $\oint_{\partial V} \mathbf{B} \cdot d\mathbf{S} = 0$
- In any case overwrite boundaries
- Difference in 2 free energy expressions=measure of divergence-freeness

$$E_{c1} - E_{c2} = \frac{-1}{4\pi} \int_{\partial V} \varphi (\mathbf{B} - \mathbf{B}_p) \cdot d\mathbf{S} + \frac{1}{4\pi} \int dV \varphi (\nabla \mathbf{B}_c)$$

$$E_{divg} = |E_{c1} - E_{c2}|$$

$$r = \frac{|E_{c1} - E_{c2}|}{|E_{c1}| + E_{c2}}$$

Volume method

step 2: Calculation of vector potentials \mathbf{A} , \mathbf{A}_p

solve $\mathbf{B} = \nabla \times \mathbf{A}$ for vector potential \mathbf{A} with the method of Valori+ 2012

DeVore gauge

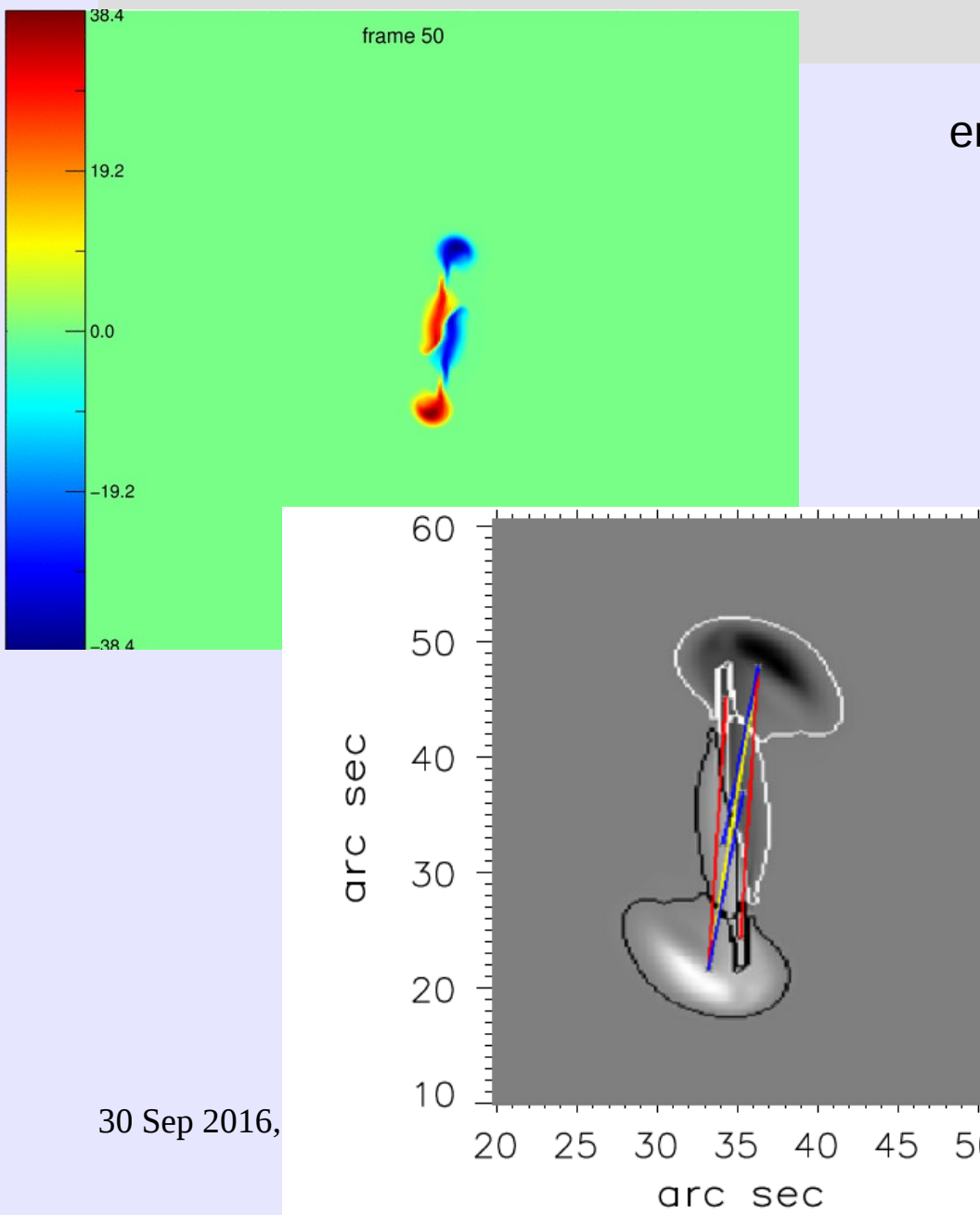
$$\hat{\mathbf{z}} \cdot \mathbf{A} = 0$$

so that

$$\left\{ \begin{array}{l} \mathbf{A} = \mathbf{A}_0 - \hat{\mathbf{z}} \times \int_{z_0}^z dz' \mathbf{B}(x, y, z') \\ \mathbf{A}_0 = \left(\frac{-1}{2} \int_{y_0}^y dy' B_z(x, y', z=z_0), \frac{1}{2} \int_{x_0}^x dx' B_z(x', y, z=z_0), 0 \right) \end{array} \right.$$

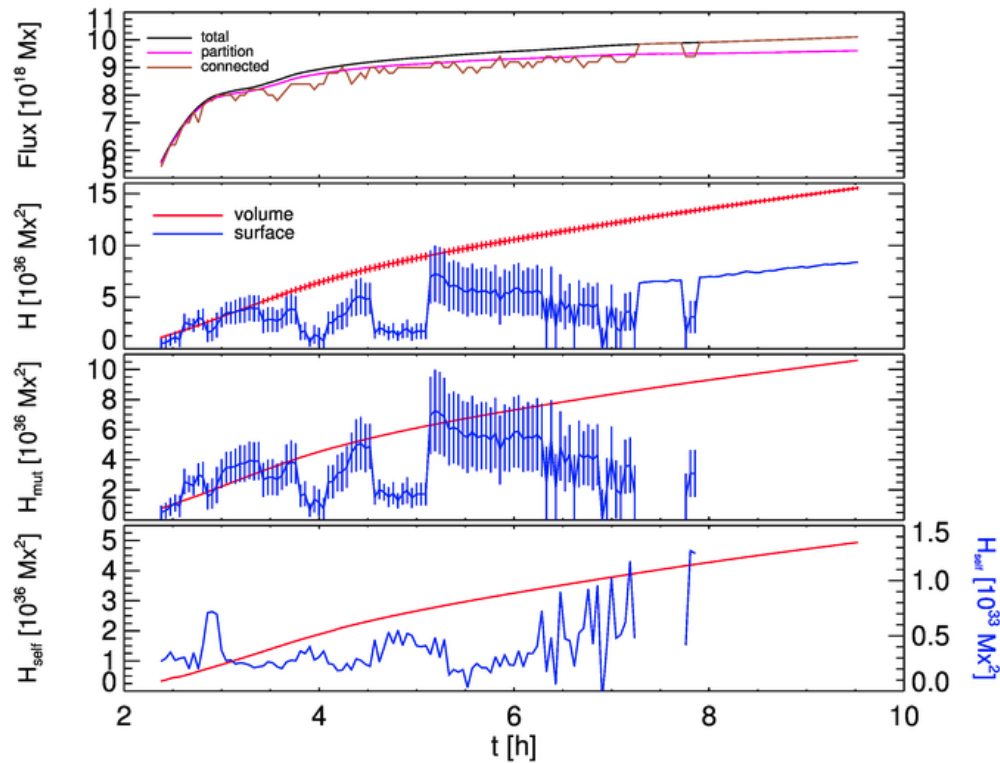
- Formulas valid for divergence-free fields
- Differentiation with 2nd order derivatives
integration modified Simpson's rule (error 1/N⁴)
- Top/bottom give different results - top is usually better

Non-eruptive synthetic AR



emergence of weakly twisted
flux-tube
data: V. Archontis
duration 9.5 h
3 min cadence
65x65x65 Mm
pixel size 0.2"

Non-eruptive synthetic AR



$$r=0.72, R=0.76$$

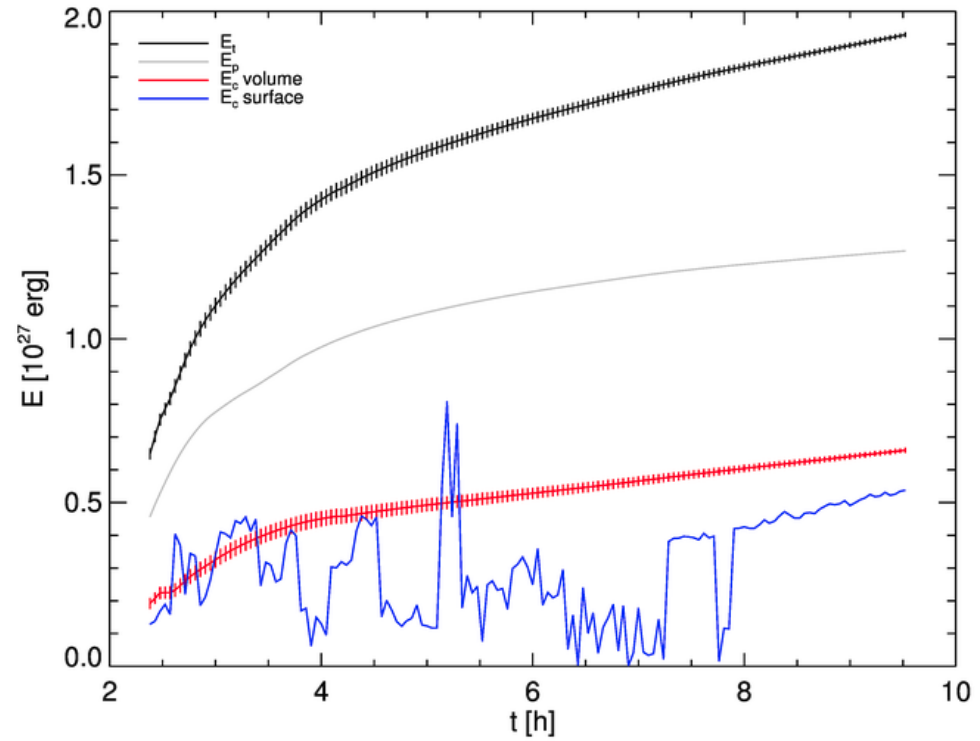
$$f=2.11 \pm 0.12$$

$$r=0.38, R=0.35$$

$$f=1.96 \pm 0.21$$

30 Sep 2016, Meudon

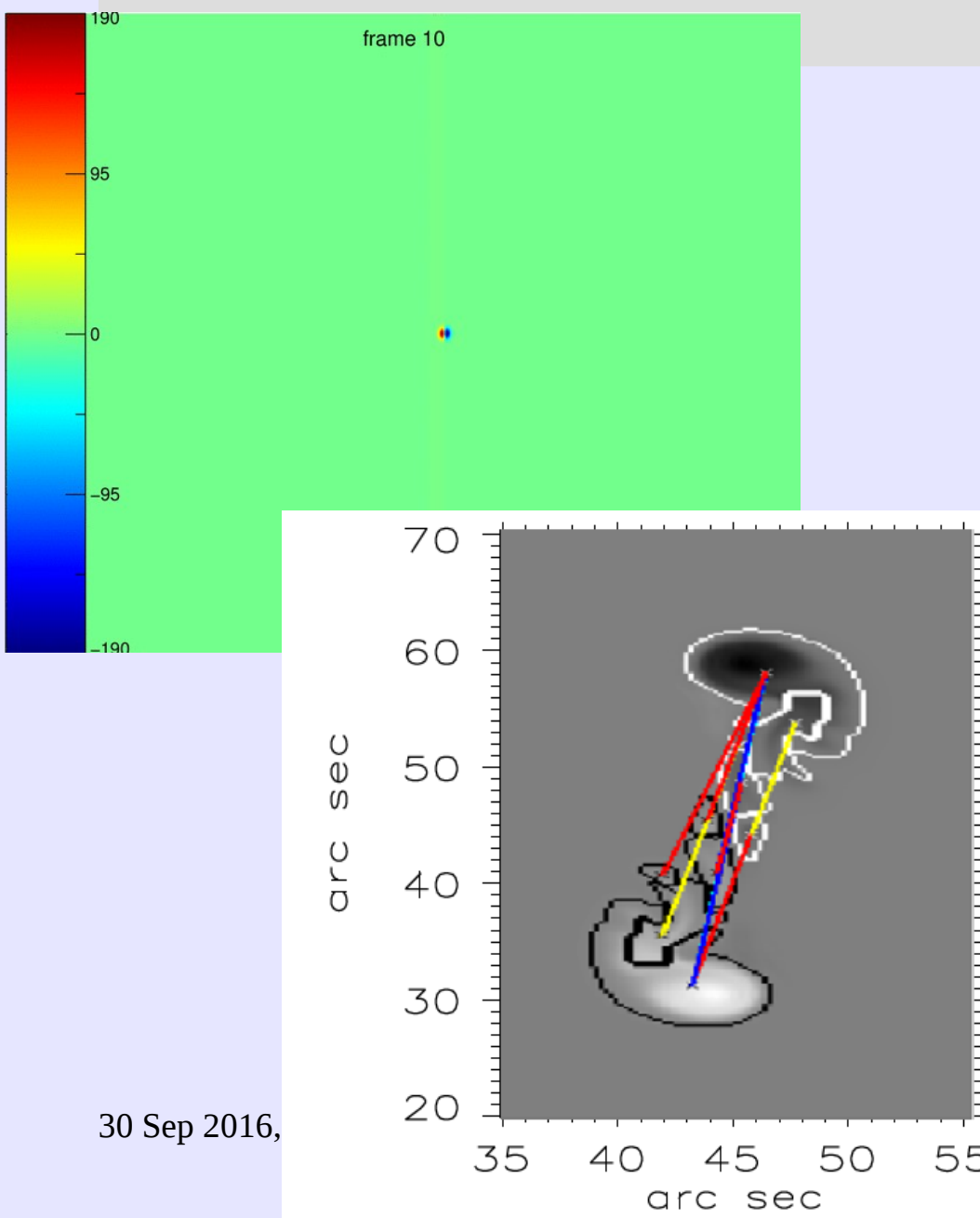
$$\begin{aligned} r &= 0.34, R = 0.29 \\ f &= (8.0 \pm 1.0) \times 10^3 \end{aligned}$$



$$r=0.26, R=0.38$$

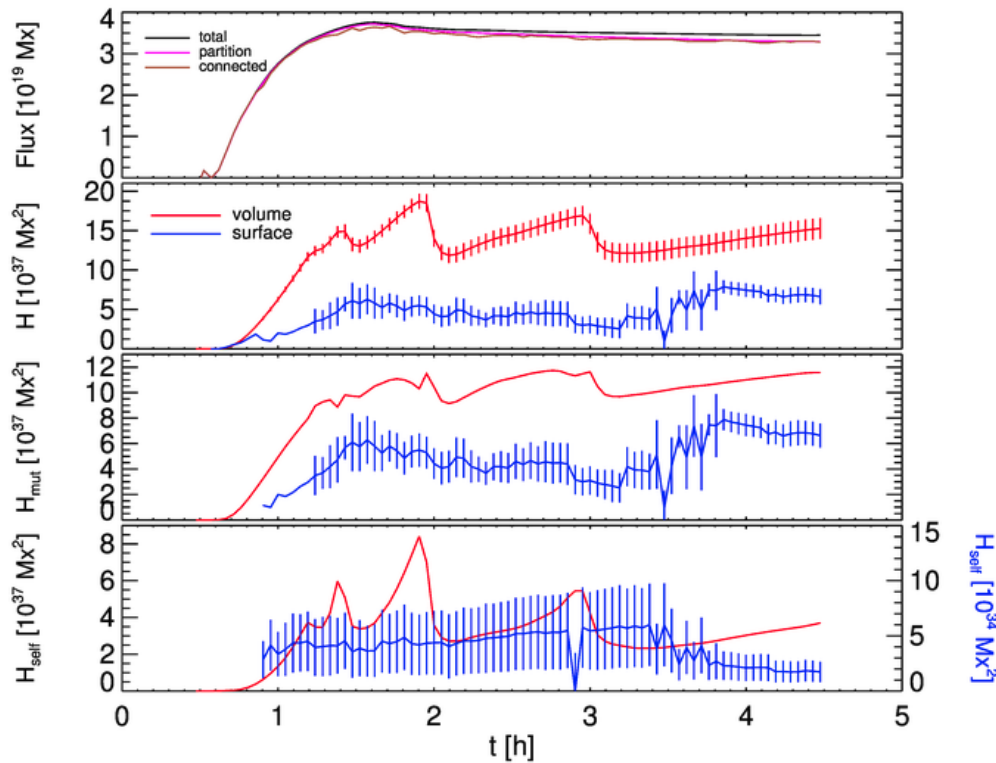
$$f=1.66 \pm 0.14$$

Eruptive synthetic AR



emergence of more twisted
flux-tube
data: V. Archontis
duration 4.5 h
3 min cadence
65x65x65 Mm
pixel size 0.2"

Eruptive synthetic AR

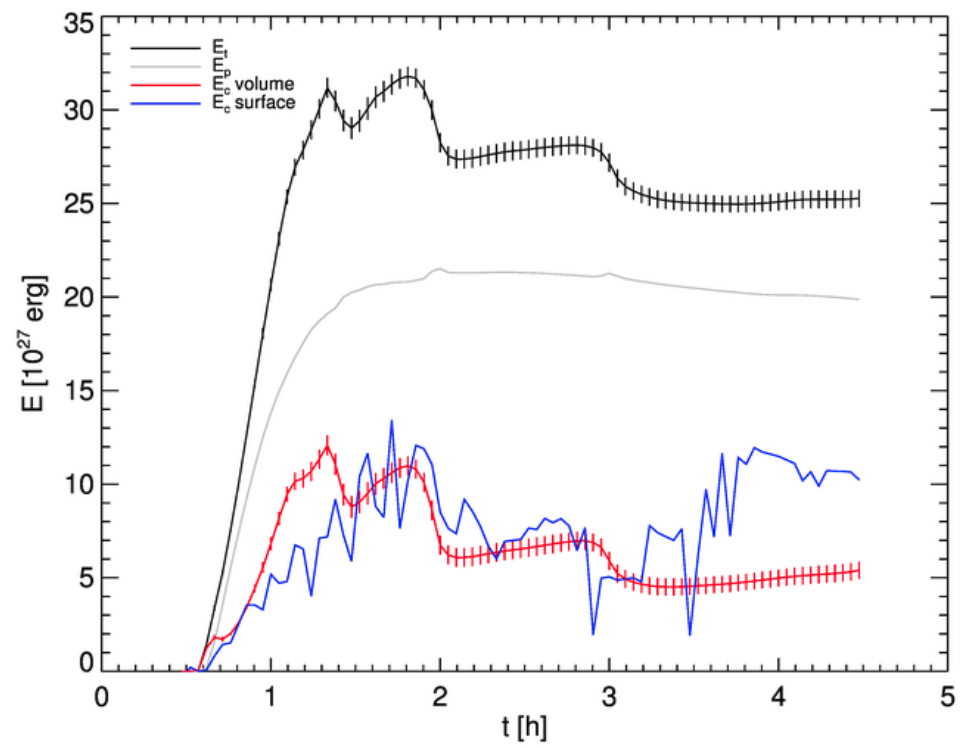


$r=0.74$, $R=0.6$
 $f=2.8 \pm 0.2$

$r=0.6$, $R=0.48$
 $f=1.91 \pm 0.19$

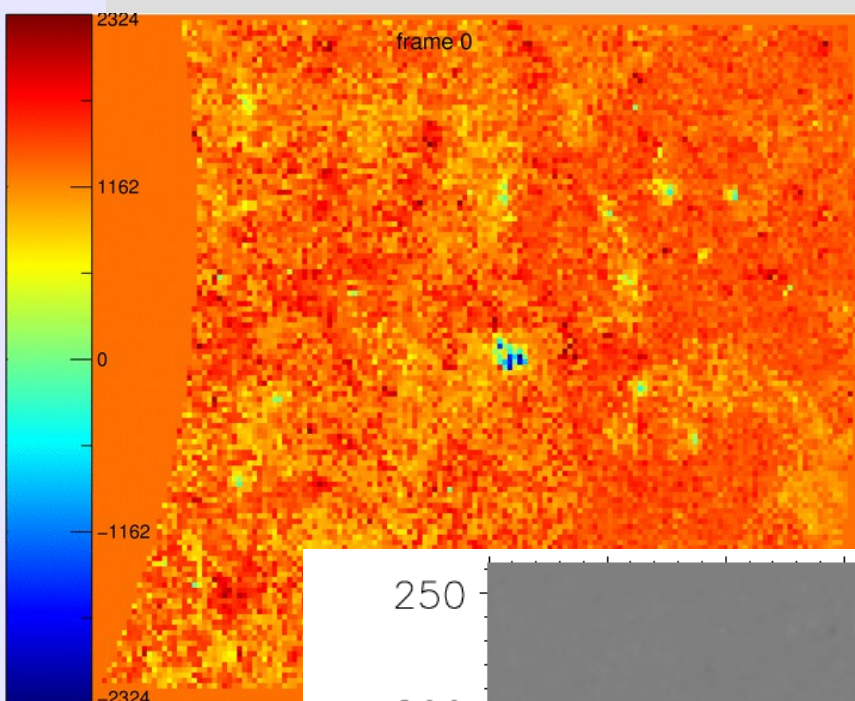
$r=0.062$, $R=-0.007$
 $f=(7.8 \pm 1.0) \times 10^2$

30 Sep 2016, Meudon

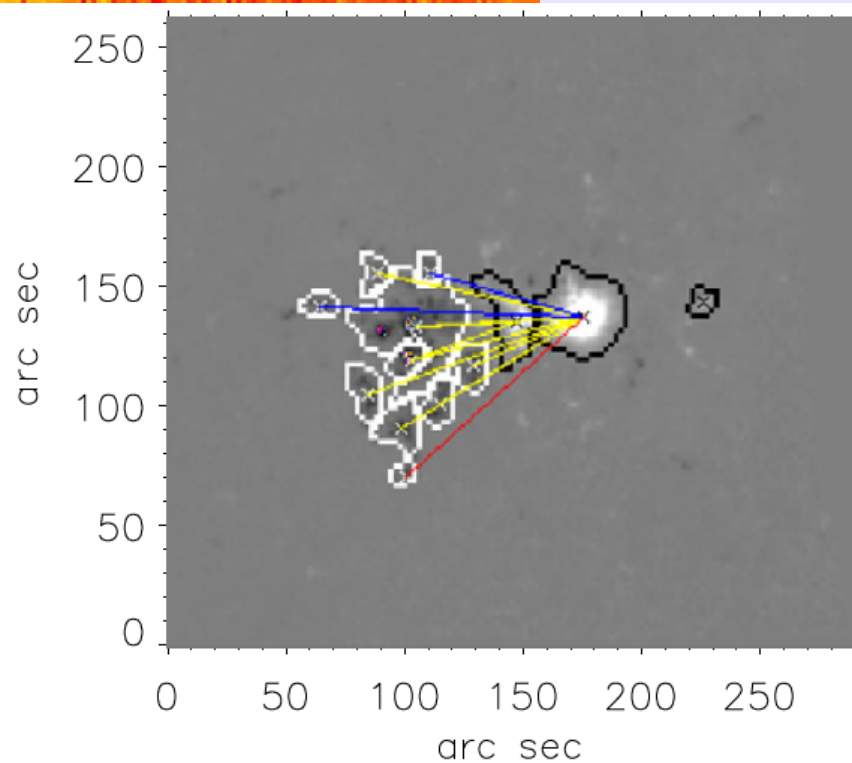


$r=0.43$, $R=0.28$
 $f=0.85 \pm 0.09$

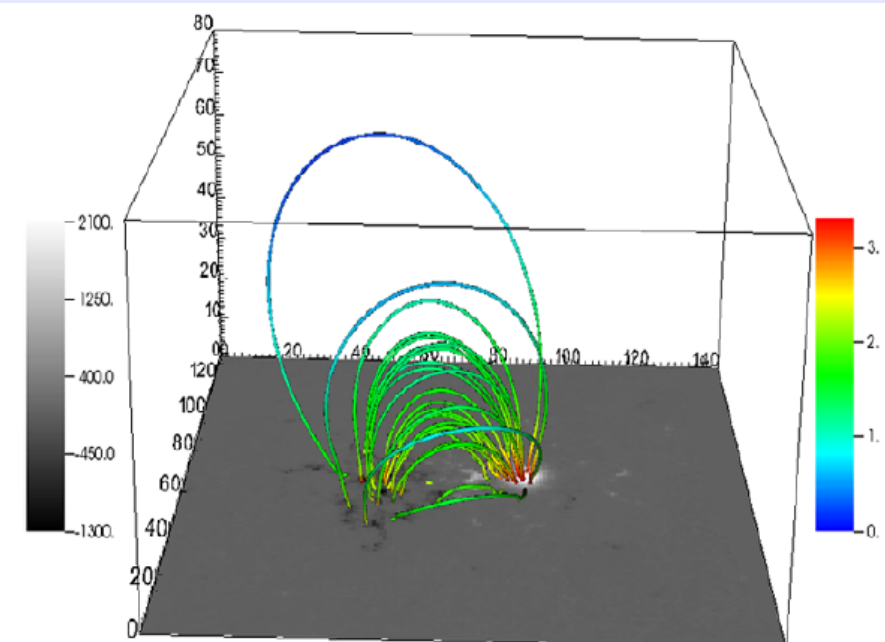
Non-eruptive NOAA AR 11072



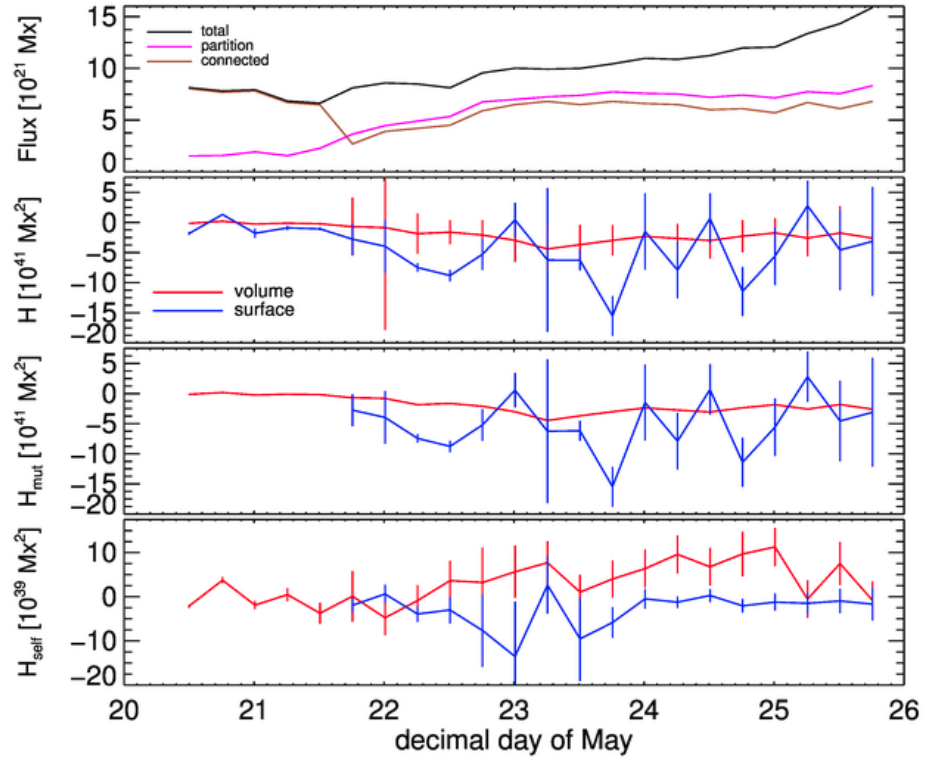
data: SDO/HMI
extrapolation: Wiegelmann 2004
(no preprocessing)
20-25 May 2010
6 h cadence
220x190x220 Mm (avg)
pixel size 2"



30 Sep 2016,



Non-eruptive NOAA AR 11072



$$r=0.35, R=0.31$$

$$f=0.45 \pm 0.25$$

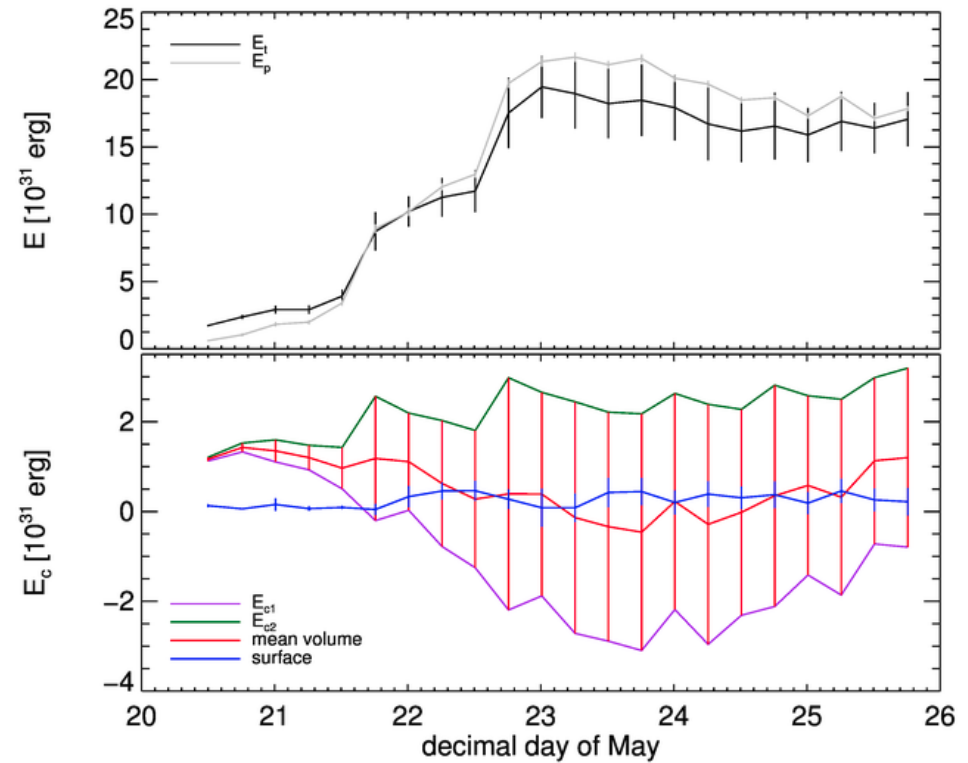
$$r=0.051, R=-0.022$$

$$f=0.37 \pm 0.24$$

30 Sep 2016, Meudon

$$r=0.11, R=0.26$$

$$f=-1.0 \pm 2.1$$

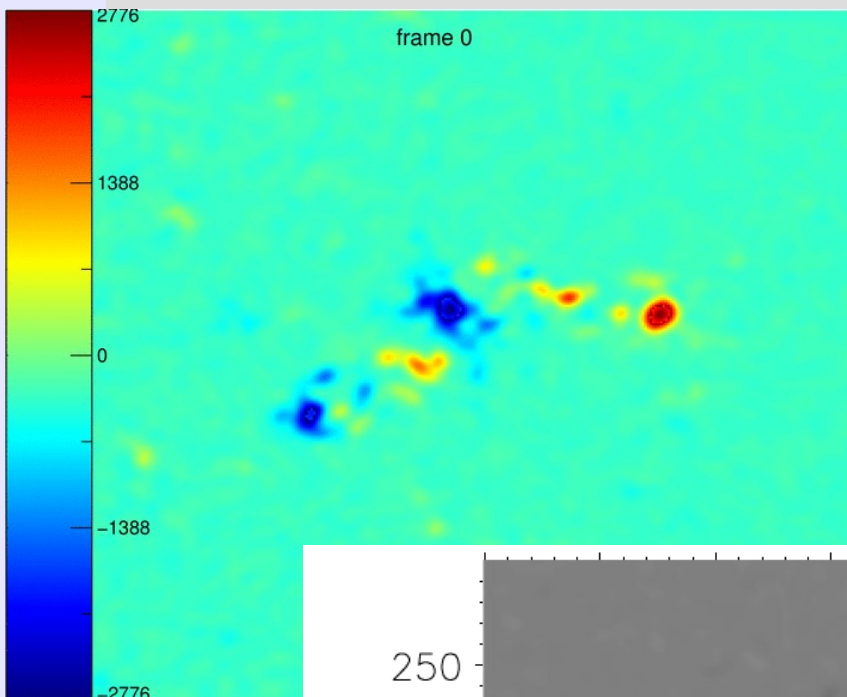


$$r=-0.57, R=-0.58$$

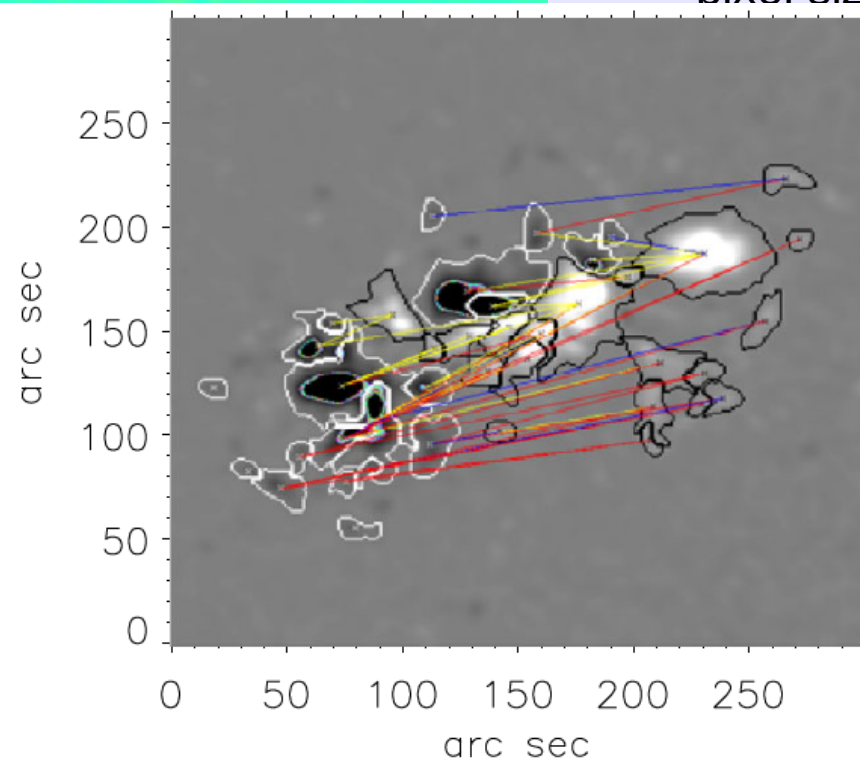
$$f=2.3 \pm 1.6$$

negative free energy!
large E_c errors!

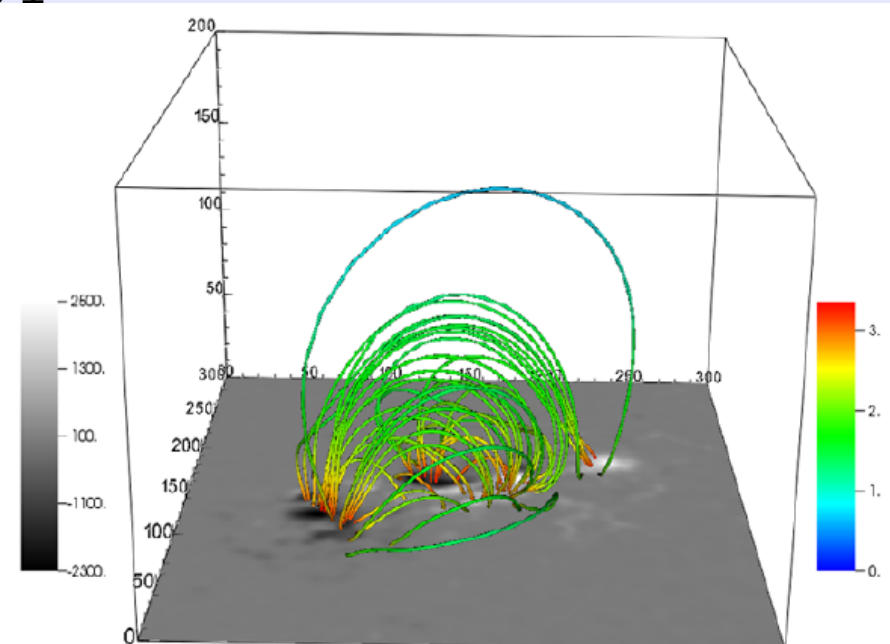
Eruptive NOAA AR 11158



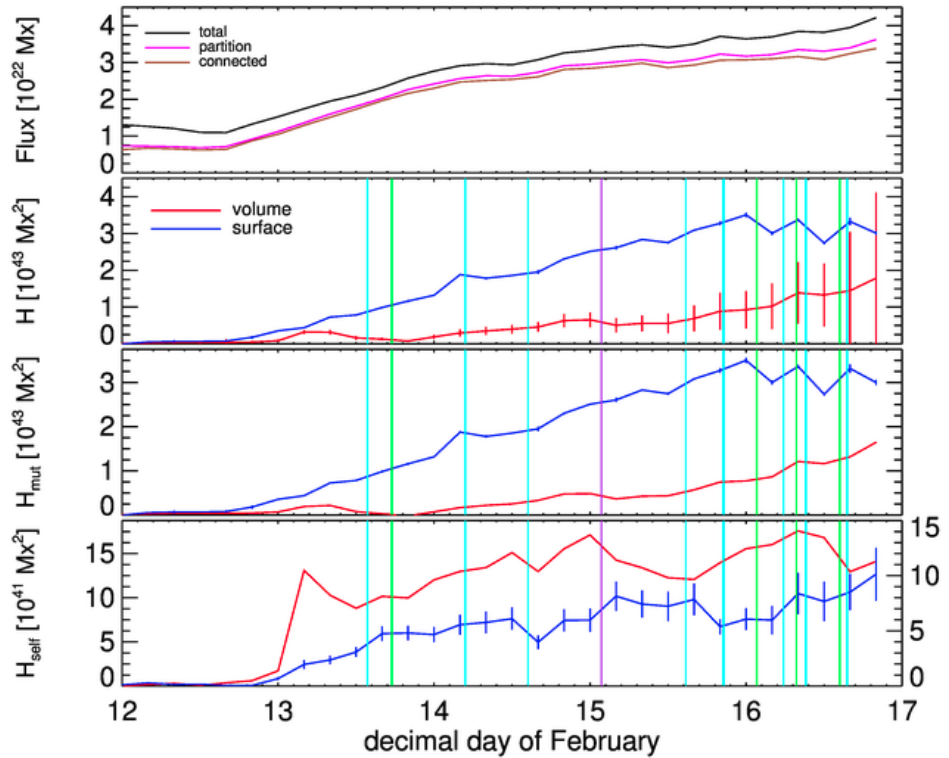
X2.2 on 15 Feb 2011, 01:44 UT
5 M-, tens C-class flares
data: SDO/HMI
extrapolation: Wiegemann 2004
(preprocessing, X. Sun)
12-16 Feb 2011
4 h cadence
216x216x184 Mm
pixel size 1"



30 Sep 2016,



Eruptive NOAA AR 11158



$$r=0.84, R=0.94$$

$$f=0.30 \pm 0.06$$

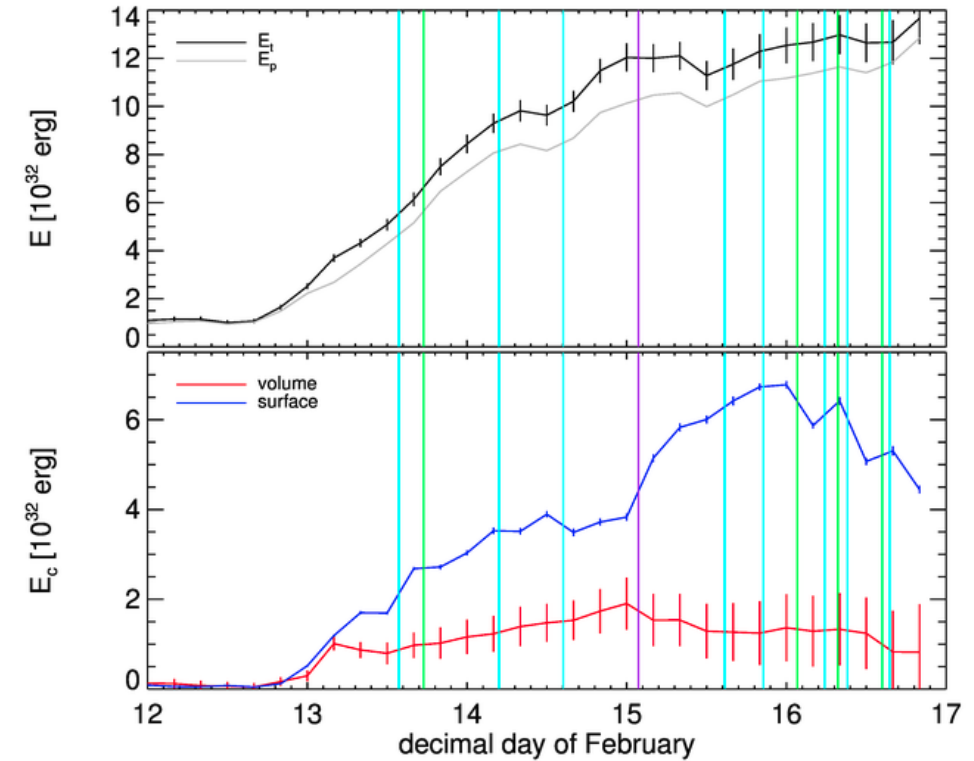
$$r=0.8, R=0.9$$

$$f=0.24 \pm 0.06$$

30 Sep 2016, Meudon

$$r=0.86, R=0.77$$

$$f=23 \pm 3$$

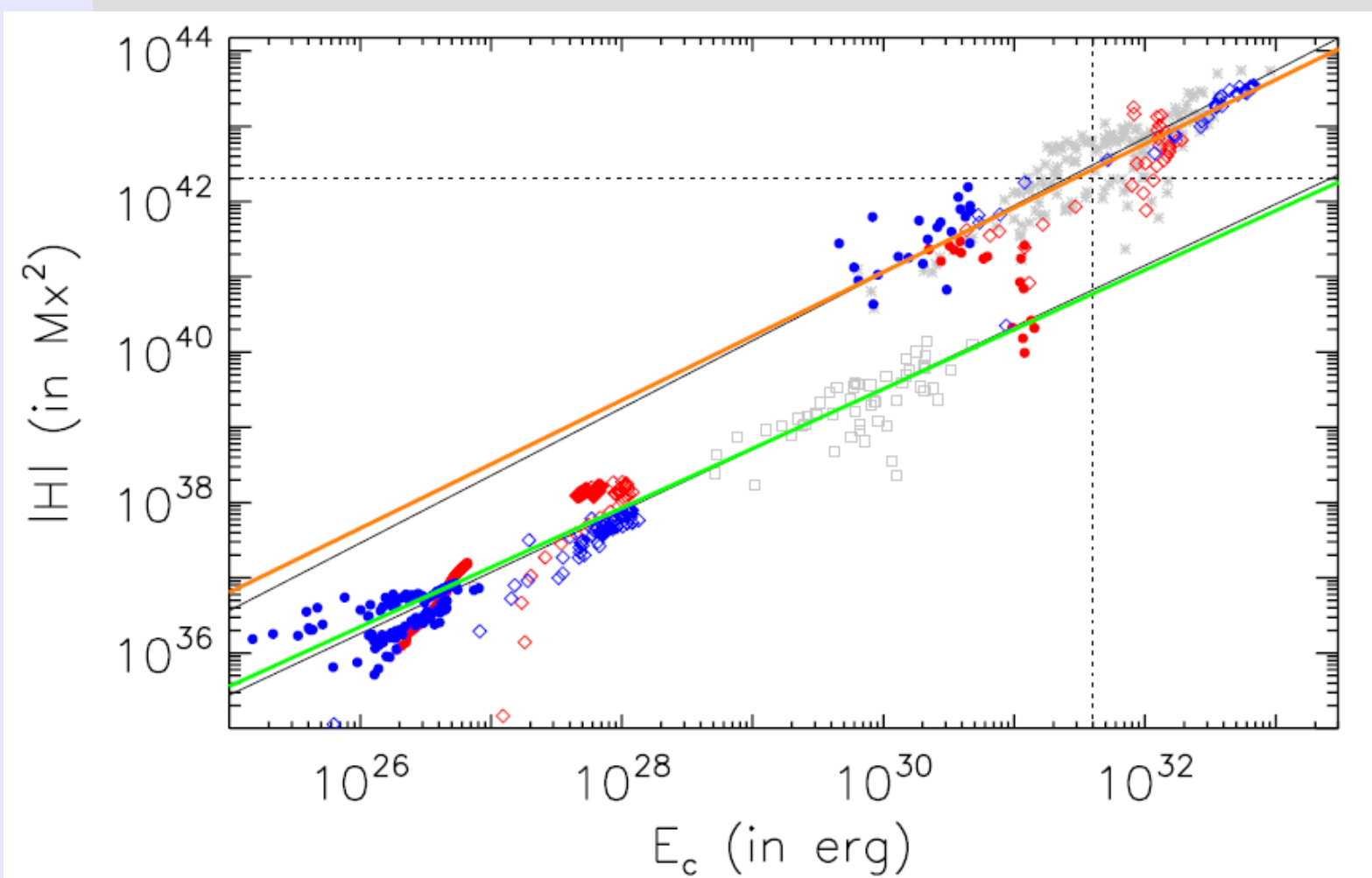


$$r=0.78, R=0.72$$

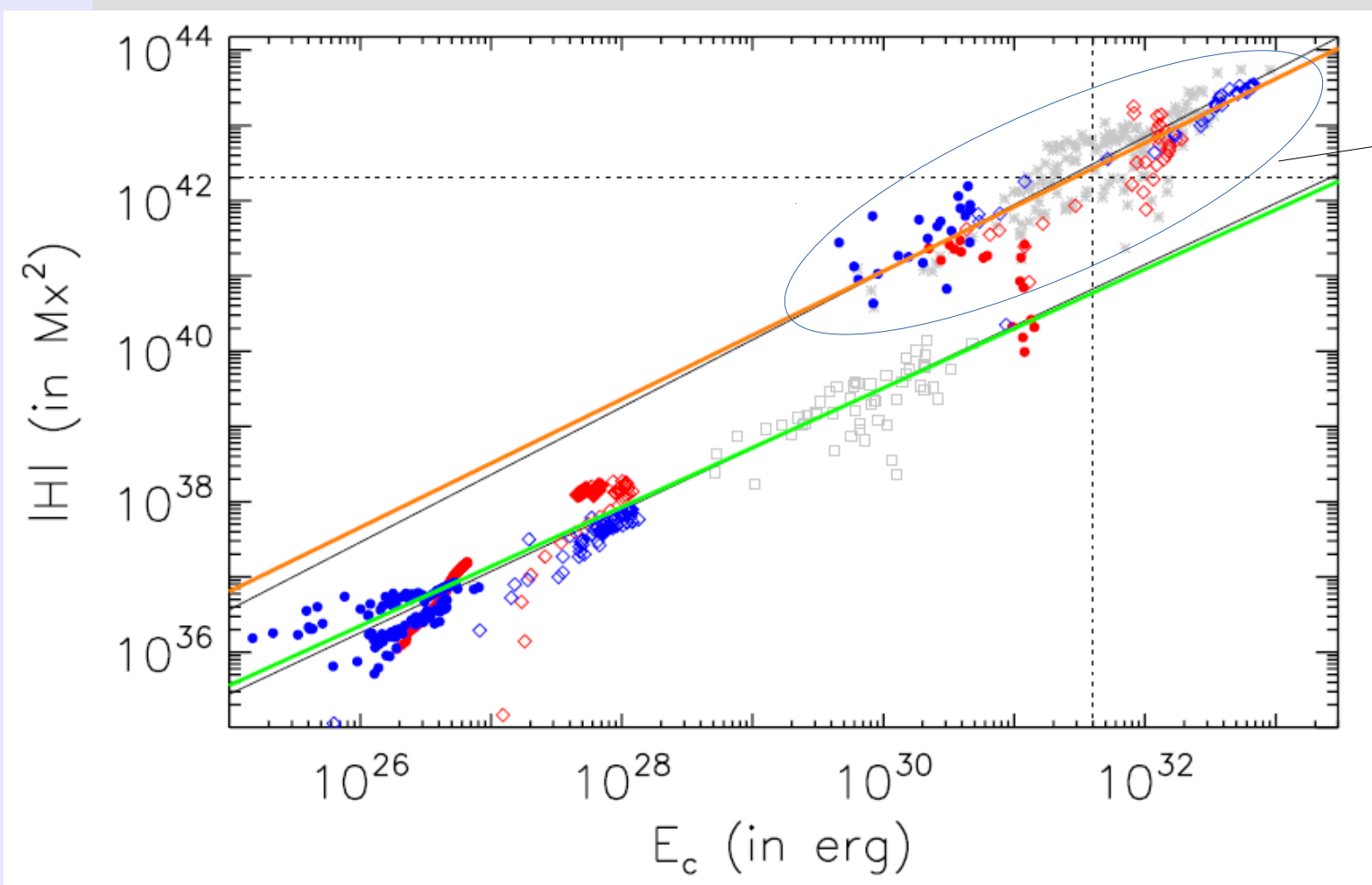
$$f=0.30 \pm 0.05$$

volume E_c below
lower-limit free energy!
Moraitis+ 2014

Energy-helicity diagram

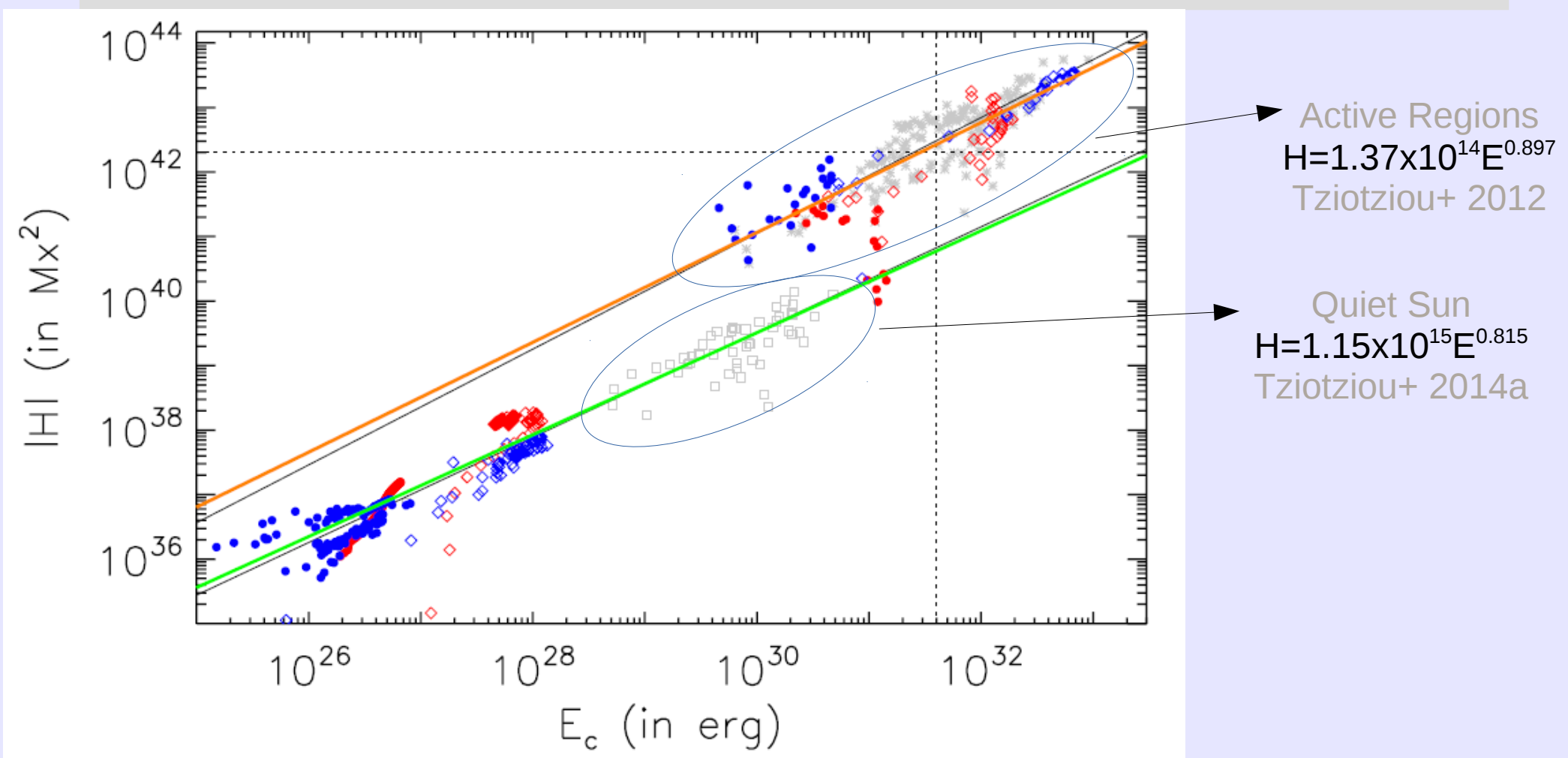


Energy-helicity diagram

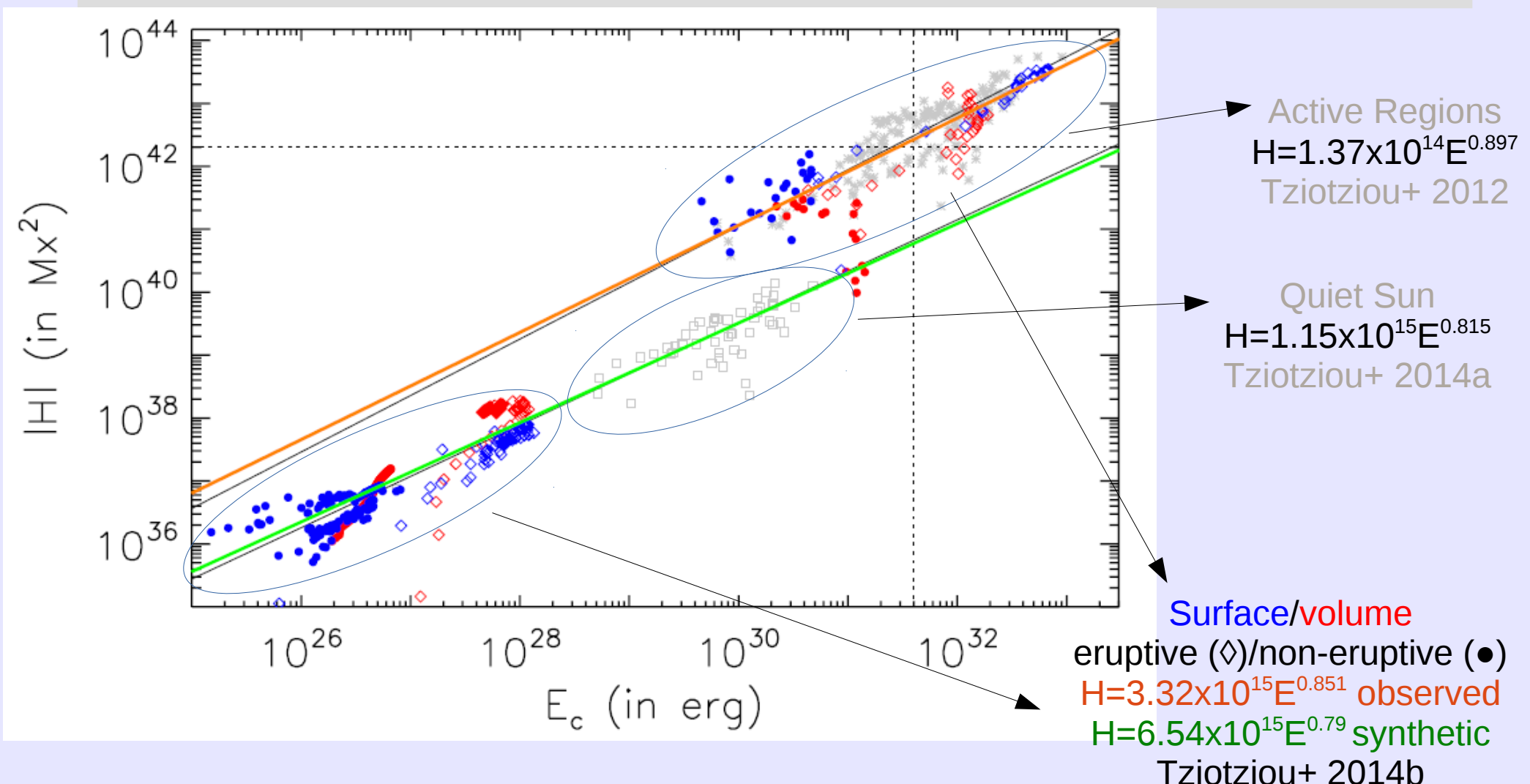


Active Regions
 $H = 1.37 \times 10^{14} E^{0.897}$
Tziotziou+ 2012

Energy-helicity diagram

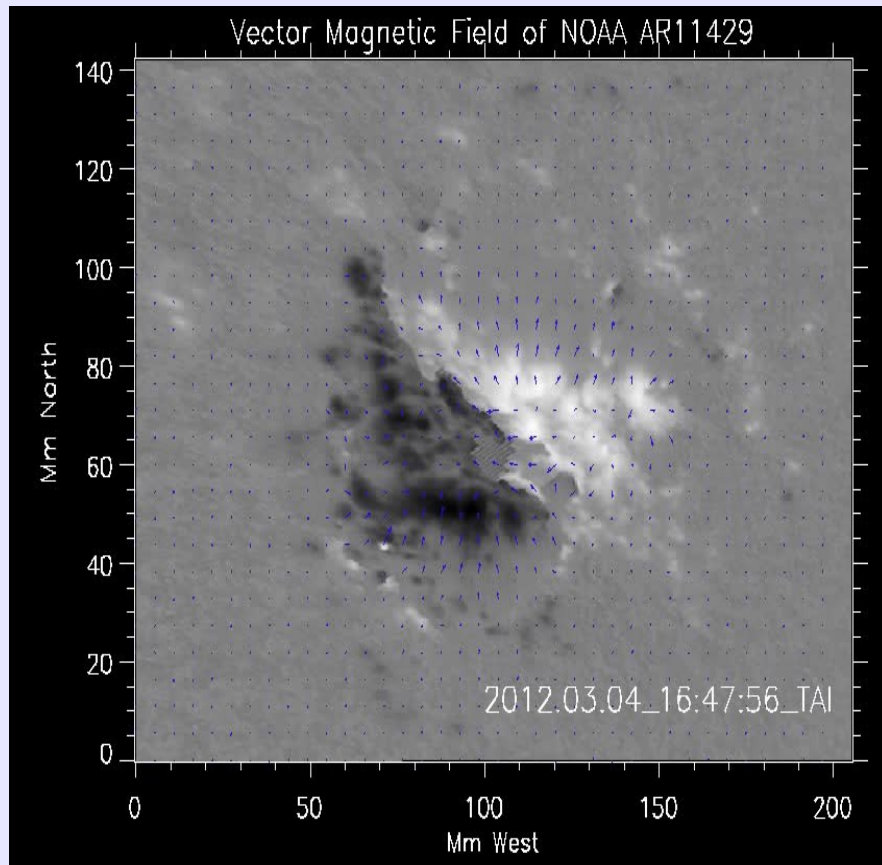


Energy-helicity diagram



NOAA AR 11429

Helicity ejection



G. Hintzoglou

Origin of intense space weather phenomena
during 7-11 March 2012

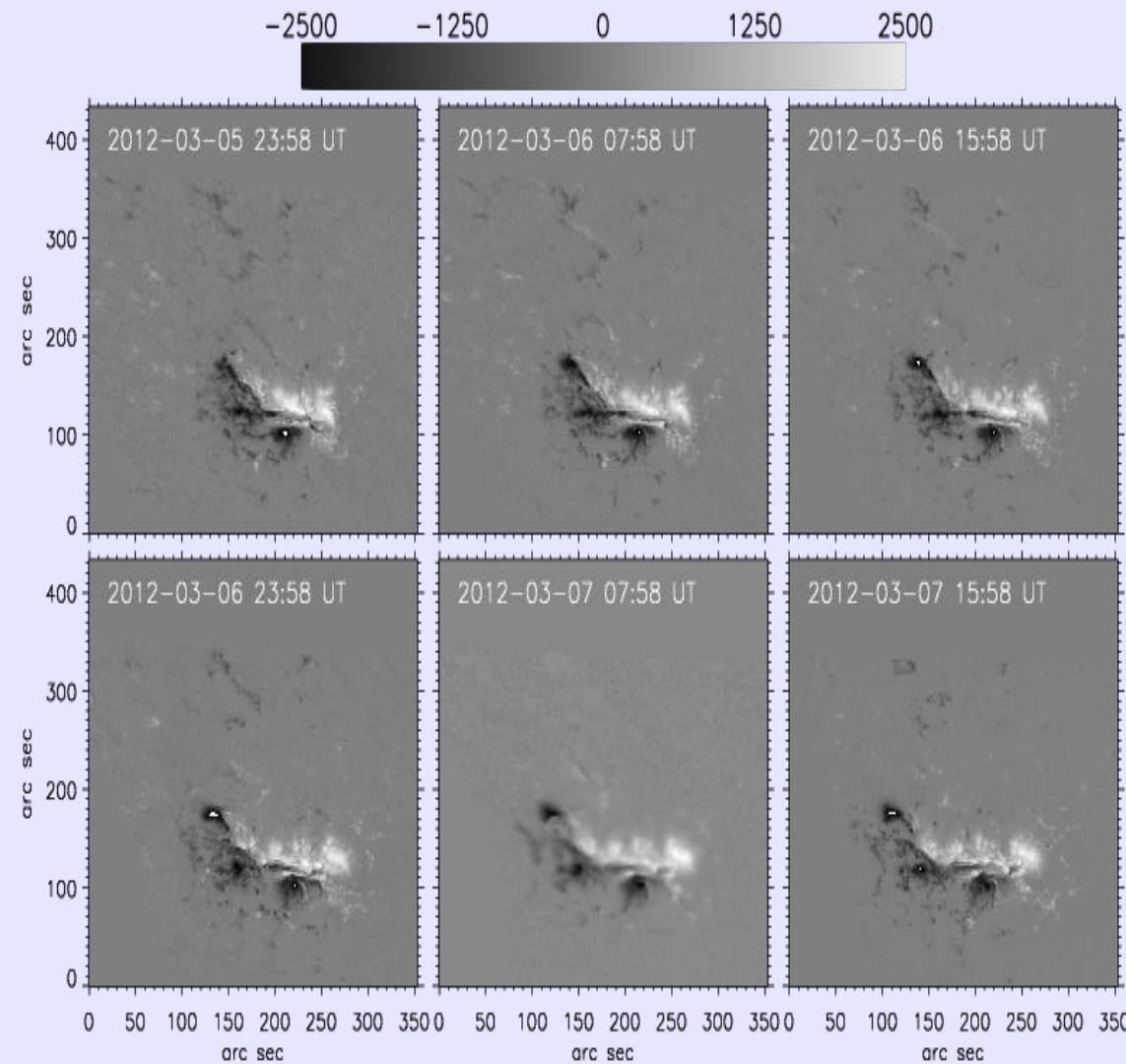
- X5.4-X1.3 flares within an hour
- Two ultra-fast CMEs ($>2000 \text{ km s}^{-1}$)
- Interplanetary CME
- Major SEP event
- Significant ULF wave enhancements and relativistic electron dropouts in the RBs
- Strong energetic-electron injection in the magnetosphere - Aurorae
- 2nd most intense geomagnetic storm of SC24

Target of HNSWRN, Patsourakos+ 2016

Period of study: 6-7 Mar 2012 (centered on X- flares)

NOAA AR 11429

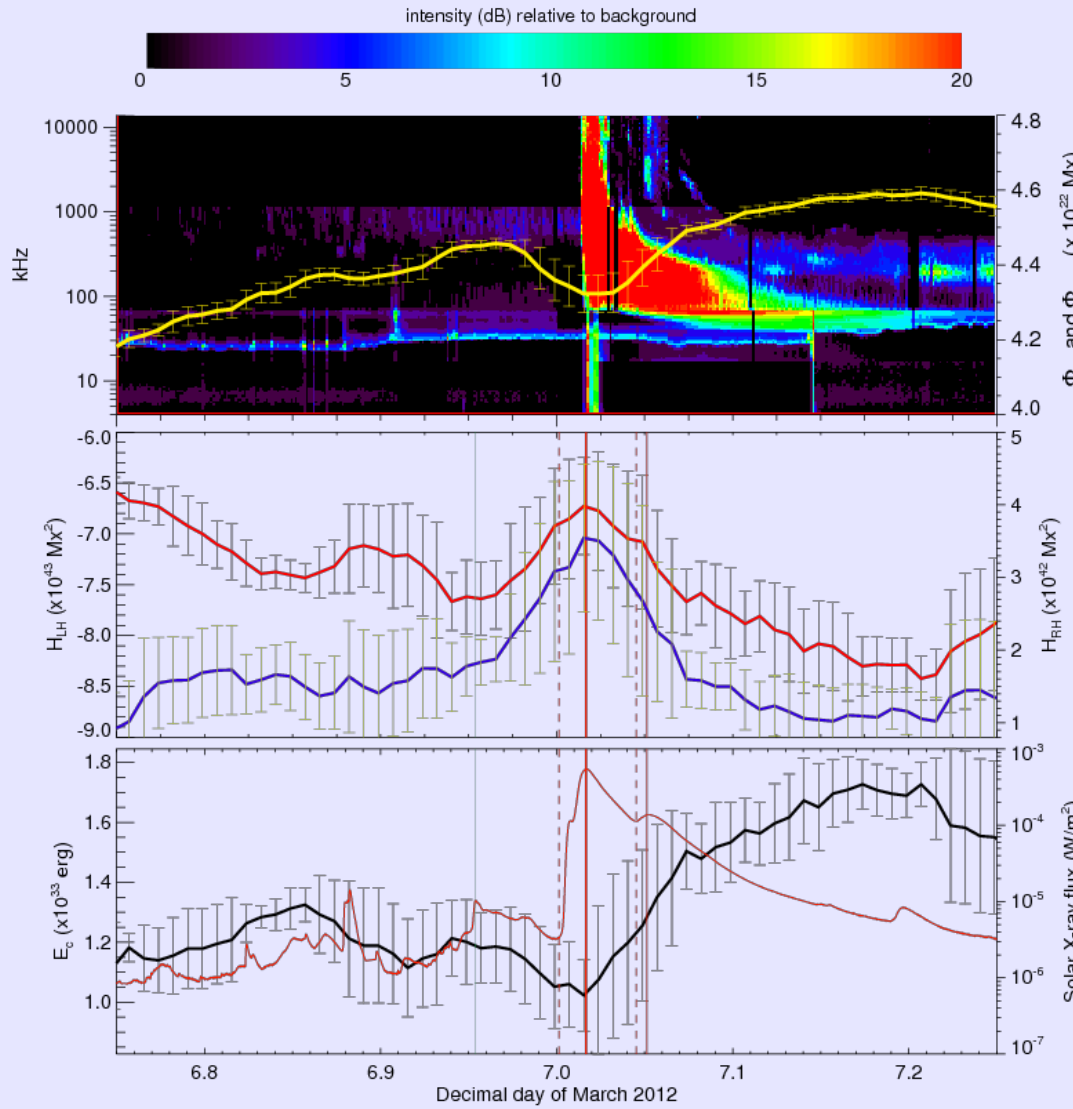
CB method



From SDO/HMI magnetograms
Take LOS magnetic field components:
create synthetic Stokes profiles (U, Q, V)
bin them by a factor of 2 (pixel size~1")
invert and obtain binned LOS magnetic
field components
Resolve 180° ambiguity
De-project onto heliographic plane
Coaling the derived data cubes
Apply free energy-helicity formulas

NOAA AR 11429

CB method



Apparent eruption-related decrease in connected flux:
reorganization of magnetic connectivity?
white-light flare emission contamination?

LH helicity: decrease of $\sim 8 \times 10^{42}$ Mx 2
attributed to 1st eruption

RH helicity: increase of $\sim 2 \times 10^{42}$ Mx 2
during 1st eruption
decrease of $\sim 2 \times 10^{42}$ Mx 2 during 2nd
Total helicity ejection $2-4 \times 10^{42}$ Mx 2

Free energy decrease of $\sim 2.5 \times 10^{32}$ erg

Sizable errors

Eruption-related changes of energy/helicity consistent with size of eruptions

NOAA AR 11429

FI method

$$\frac{dH}{dt} = 2 \int_S dS [(\mathbf{A}_p \cdot \mathbf{B}_t) v_n - (\mathbf{A}_p \cdot \mathbf{v}_t) B_n] = \int_S dS [-2(\mathbf{A}_p \cdot \mathbf{u}) B_n]$$

flux transport velocity $\mathbf{u} = \mathbf{v}_t - (v_n/B_n) \mathbf{B}_t$

Berger & Field 1984

$$G_\theta(\mathbf{x}) = -\hat{\mathbf{n}} \cdot \frac{B_n(\mathbf{x})}{2\pi} \int_S dS' \left\{ \frac{\mathbf{x} - \mathbf{x}'}{|\mathbf{x} - \mathbf{x}'|^2} \times [\mathbf{u}(\mathbf{x}) - \mathbf{u}(\mathbf{x}')] \right\} B_n(\mathbf{x}')$$

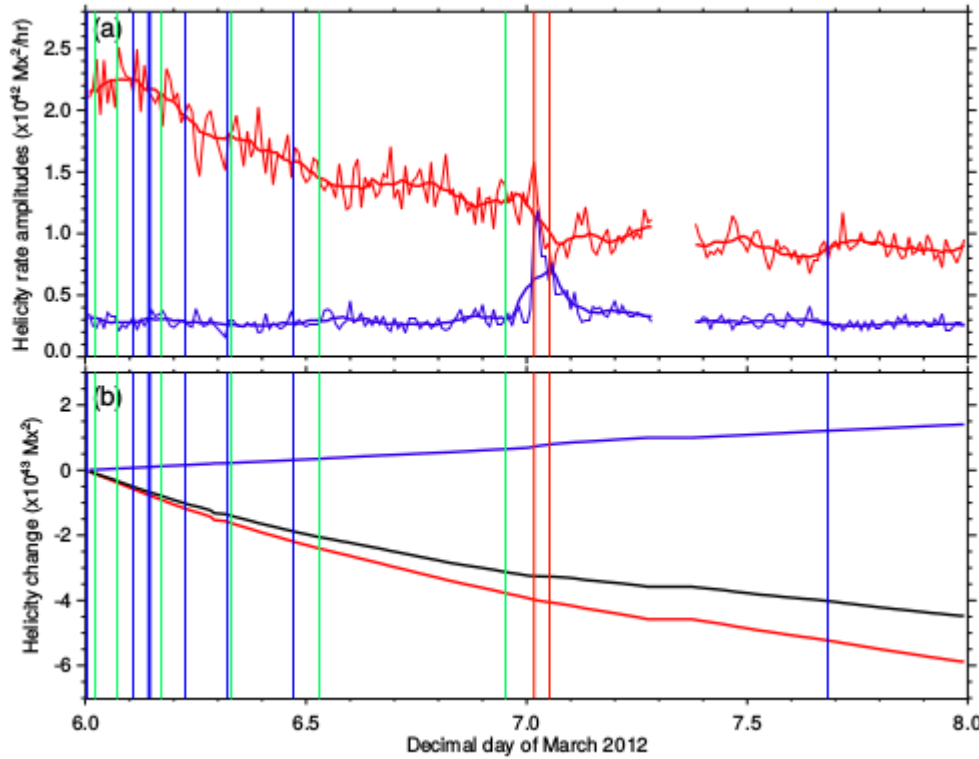
Pariat+ 2005
Liu & Schuck 2013

From SDO/HMI sequence of vector magnetograms

- Disambiguated
- Converted to cylindrical equal area maps
- Compute horizontal velocities using DAVE4VM (Schuck 2008) – normal component of the ideal induction equation
- Removed field-aligned plasma flow
- Calculate G_θ

NOAA AR 11429

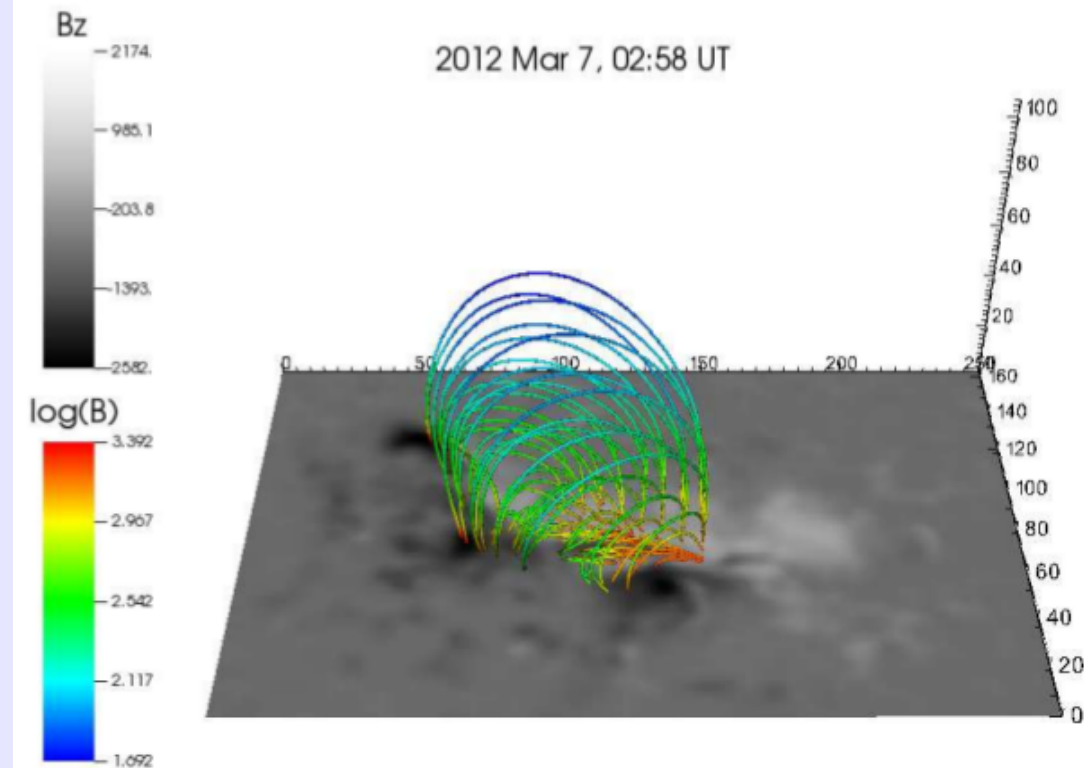
FI method



- Larger helicity injection before the flares than after
- Dominant helicity flux negative for both events
- Helicity budgets for:
 - 1st eruption $-3.3 \times 10^{43} \text{ Mx}^2$
 - 2nd eruption $-2.2 \times 10^{43} \text{ Mx}^2$
 - both eruptions $\sim 3-3.5 \times 10^{43} \text{ Mx}^2$

NOAA AR 11429

FV method



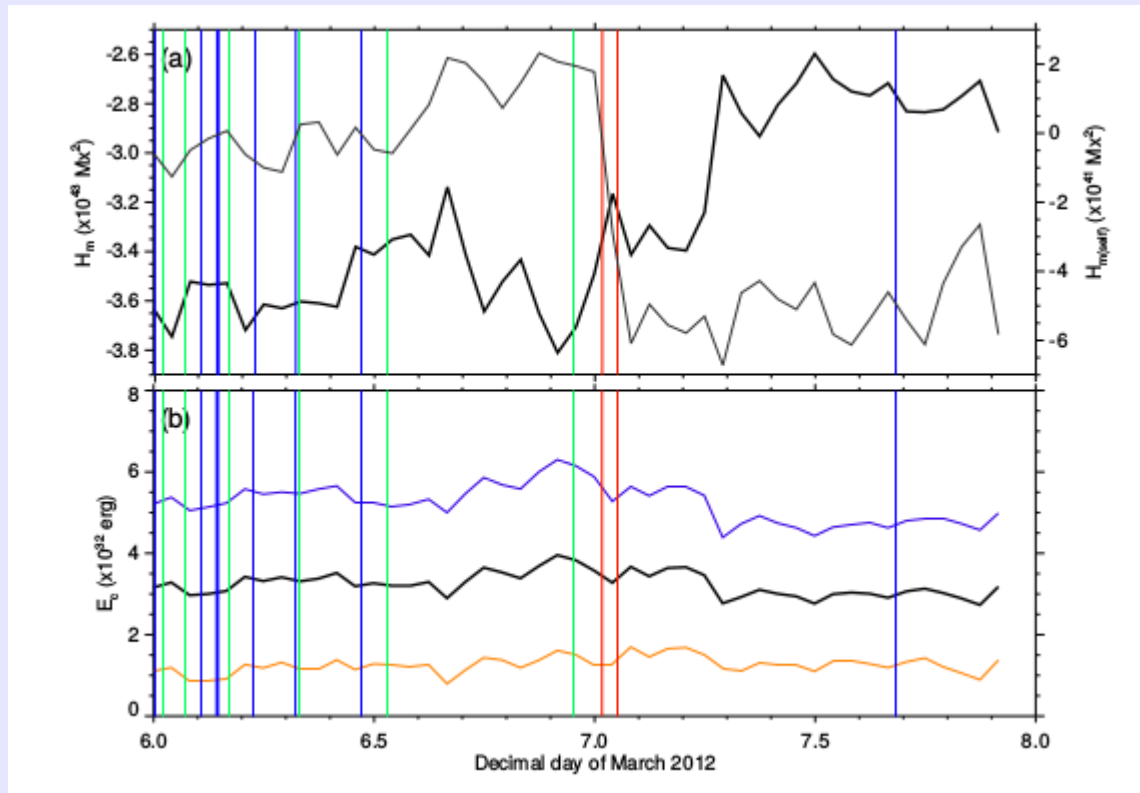
SDO/HMI vector magnetogram data

- Disambiguated
- Converted to cylindrical equal area maps
- Rebin to 720 km/pixel
- Preprocess (Wiegelmßann & Inhester 2006)
- Extrapolate 3D field
(Wiegelmßann 2004 code)



47 snapshots of the 3D field
(250x163x106 grid)
starting 5 March 2012 23:58 UT
with one hour cadence (Hintzoglou+ 2015)

NOAA AR 11429 FV method



left-handed
decrease $\Delta H \sim 8 \times 10^{42} \text{ Mx}^2$

right to left-handed
change $\Delta H \sim 6 \times 10^{41} \text{ Mx}^2$

little variation
mean $E_c \sim 3 \times 10^{32} \text{ erg}$
factor ~ 5 between E_c 's
factor ~ 3 below connectivity
method

limited NLFFF extrapolation quality
(Moraitis+ 2014)

NOAA AR 11429

Summary

| | positive helicity (Mx ²) | negative helicity (Mx ²) | net helicity (Mx ²) |
|-----------------------|---|---|---------------------------------|
| helicity integration* | 7.9x10 ⁴² | -4.1x10 ⁴³ | -3.3x10 ⁴³ |
| connectivity method | 4x10 ⁴² | -8x10 ⁴² | -4x10 ⁴² |
| volume method | | | -8x10 ⁴² |

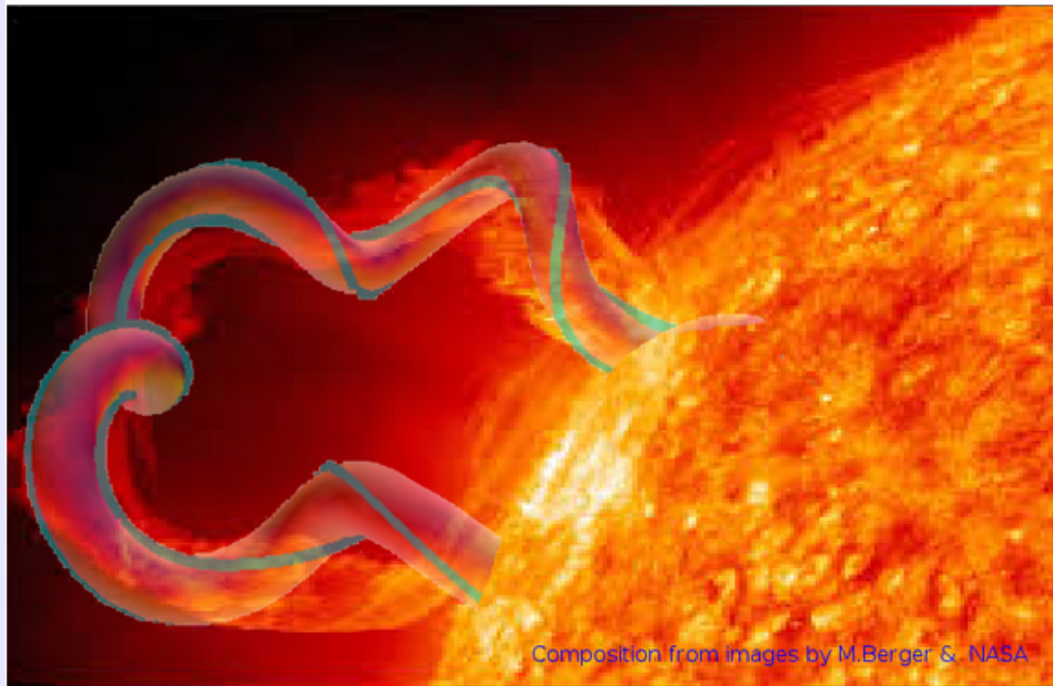
- Free energy + relative helicity evolution of AR 11429 using three different methods
- All methods agree on the sign of helicity
- Combined estimate for the eruption-related helicity changes
- Free energy + helicity budgets consistent with size of eruptions

ISSI team on magnetic helicity

Magnetic Helicity estimations in models and observations of the solar magnetic field

ISSI Team led by Gherardo Valori (MSSL - UK) & Etienne Pariat (LESIA - France)

Search



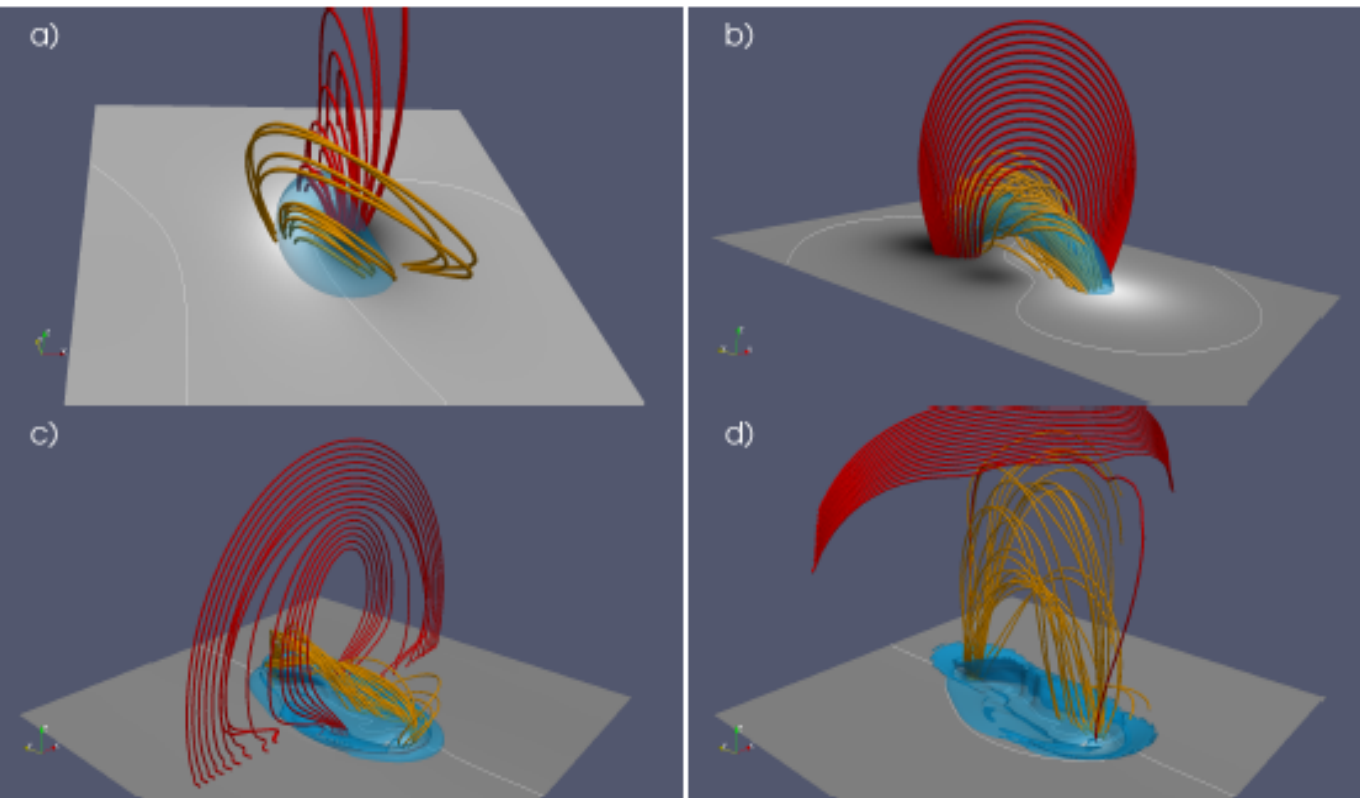
Composition from images by M.Berger & NASA



International Team on
Magnetic Helicity

ISSI team on magnetic helicity

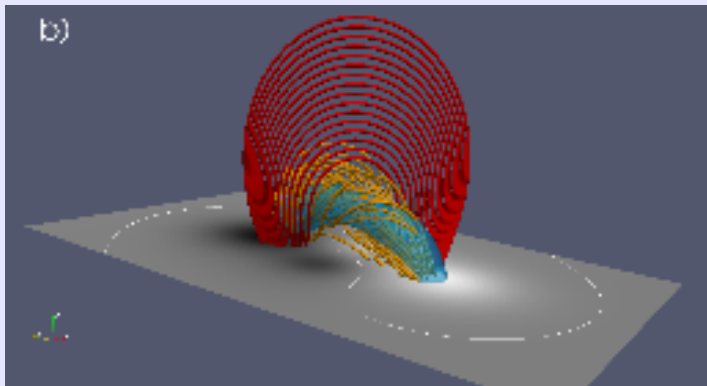
Test cases



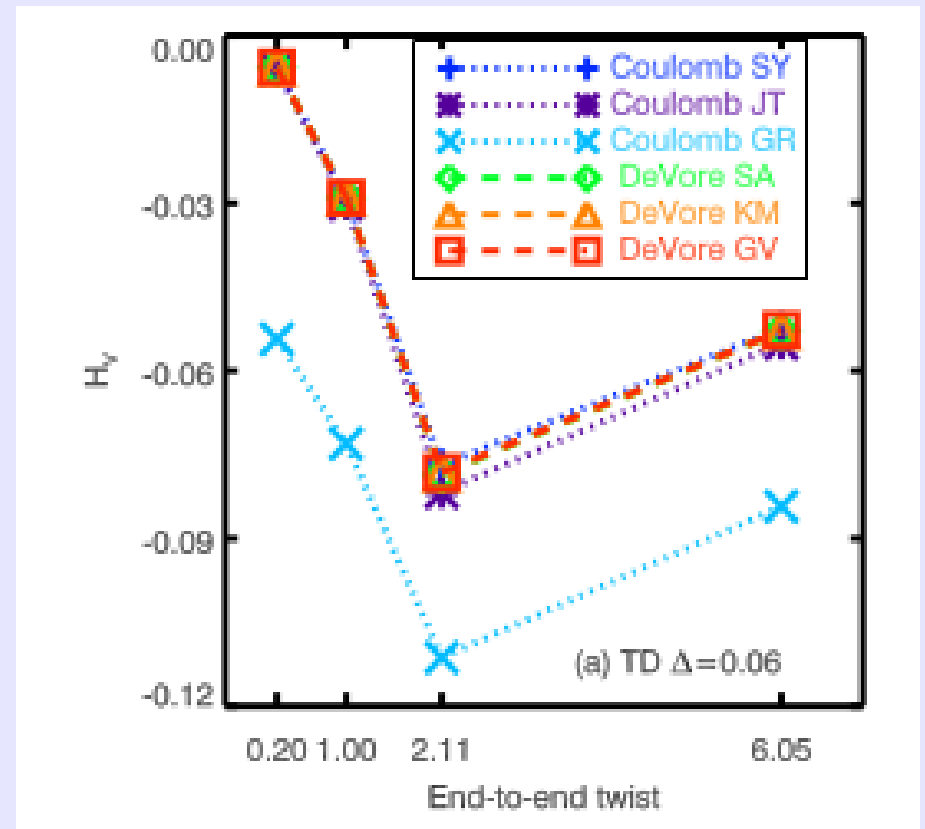
- Low & Lou @ 4 resolutions
- TD different twist and/or resolution
- Stable MHD simulation
Leake+ 2013
- Unstable MHD simulation
Leake+ 2014

ISSI team on magnetic helicity

Results - twist

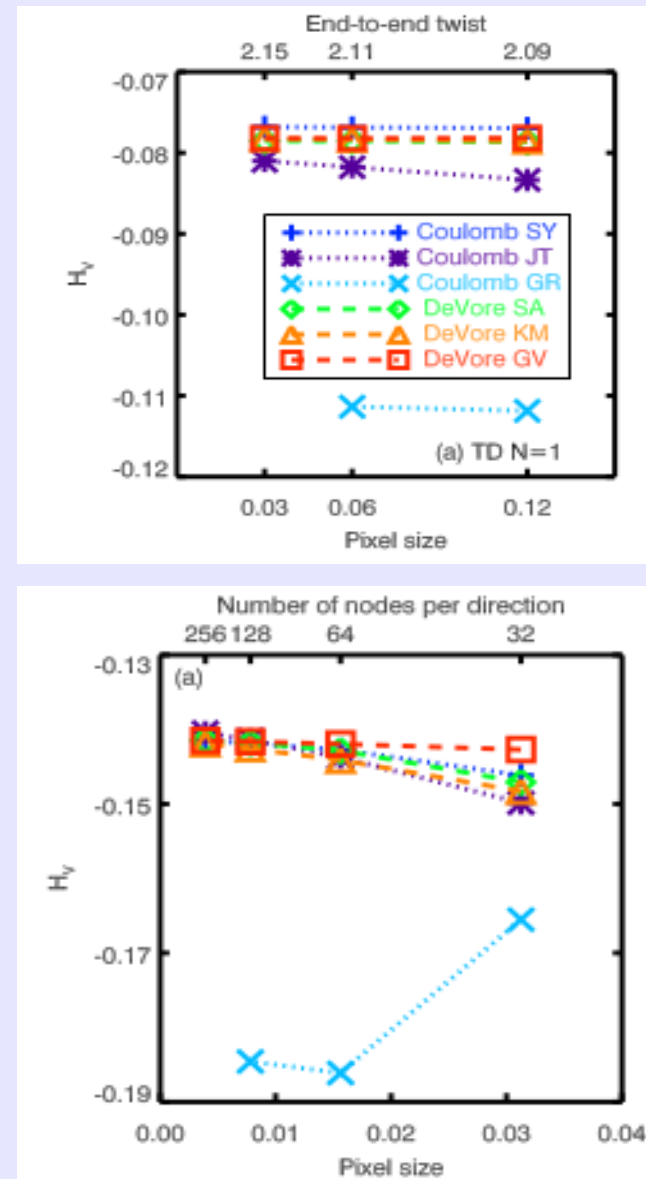
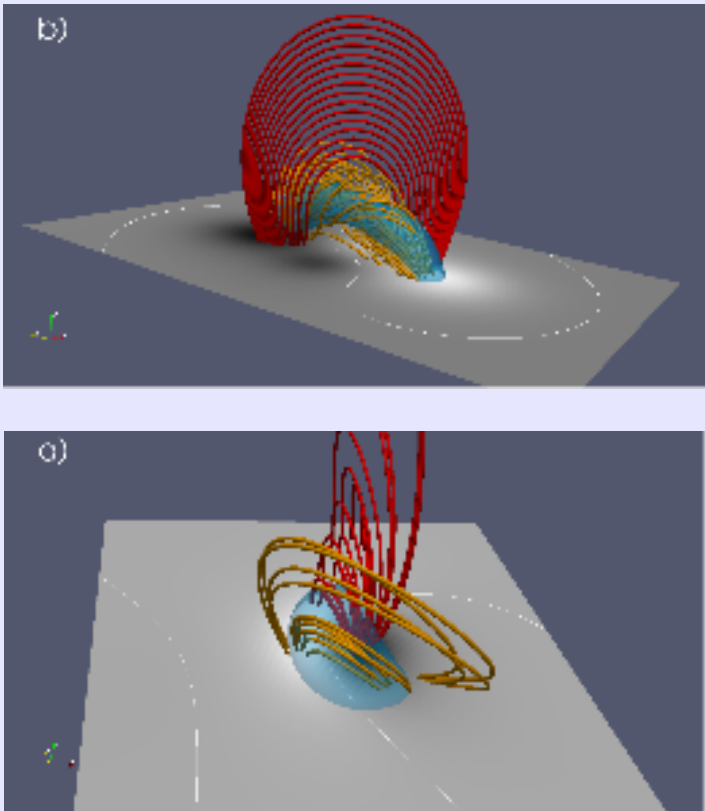


- All methods (except GR) within 2%
- DeVore more accurate than Coulomb
- More twist isn't more helicity



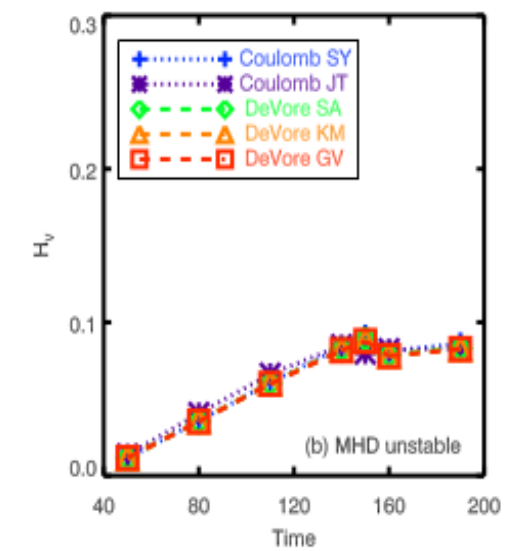
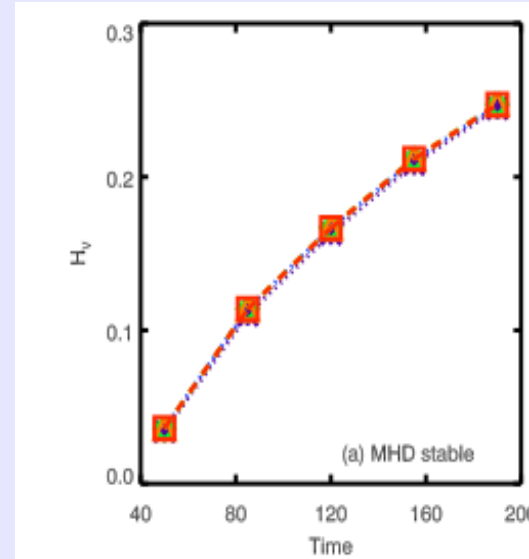
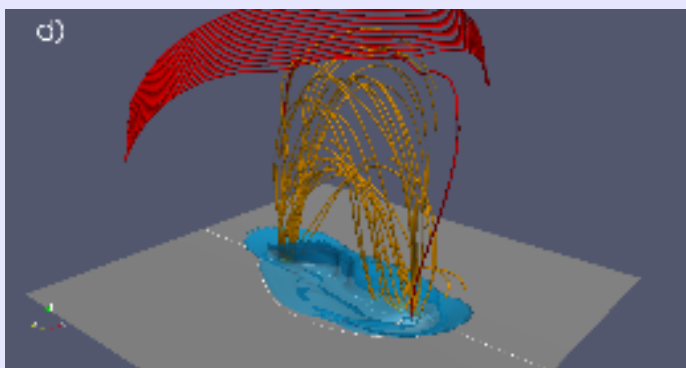
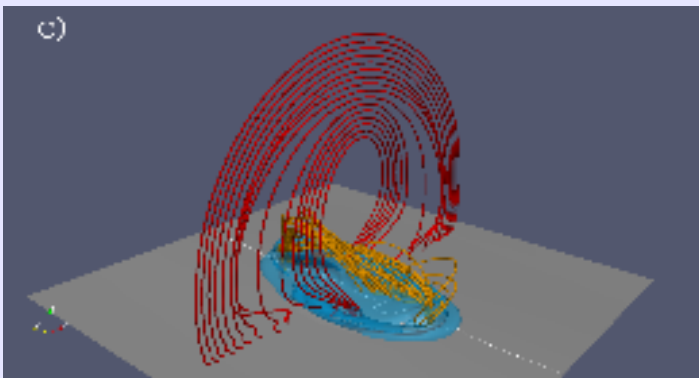
details in Valori+ 2016 (SSRv, under review)

ISSI team on magnetic helicity Results - resolution



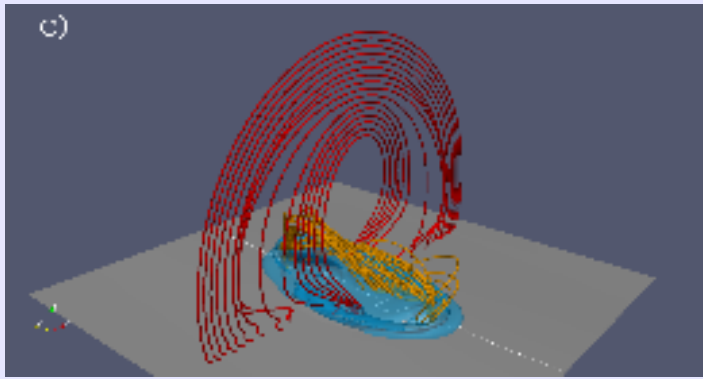
- Weak dependence on resolution in TD, but more clear in LL
- Spread within 4%
- Differences between methods more important
- Lower resolution = more B divergence

ISSI team on magnetic helicity Results - MHD



- Spread in helicity values 0.2% (st) and 3% (un)
- More helicity isn't more eruptive

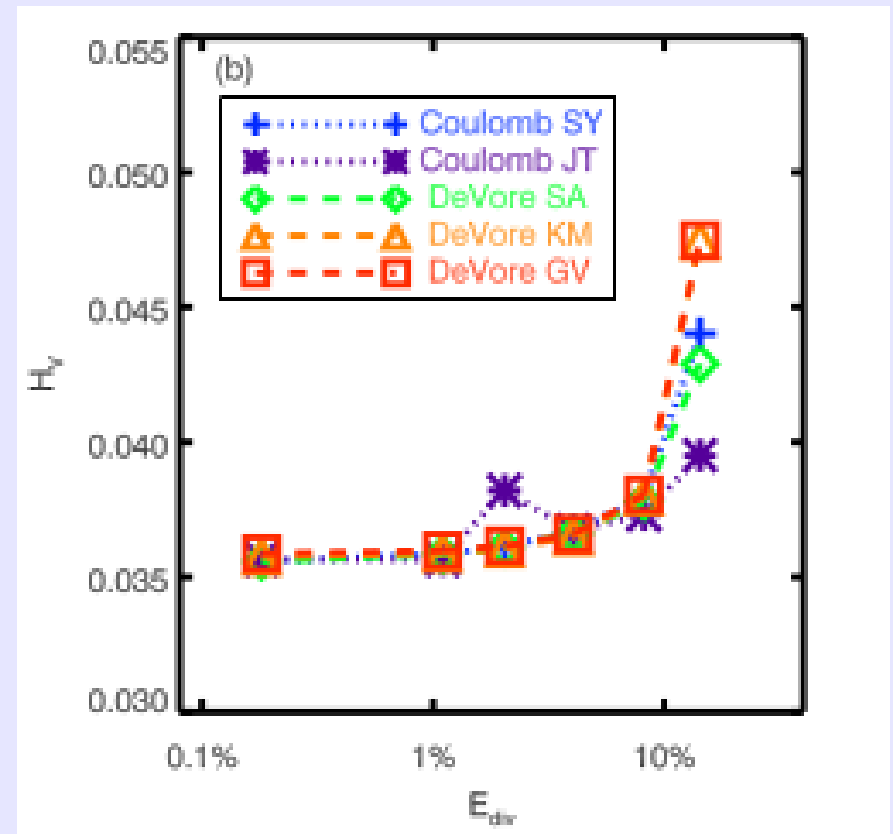
ISSI team on magnetic helicity Results - divergence



Split B (of MHD-st at t=50) in solenoidal and non-solenoidal parts (Valori+ 2013), then add ns in controlled way

$$\mathbf{B}_\delta = \mathbf{B}_s + \delta \mathbf{B}_{ns}$$

- Spread in helicity values grows from 1% to 20%
- Max reasonable helicity for divergence errors <~8%



Conclusions

- CB method within ~4 from FV, but improves if mgm ff-compatible
- Helicity is related to free energy, $H \propto E_C^{0.8-0.9}$
- Helicity is important in solar applications
- All FV methods agree to within 3%
- Small differences with resolution
- Results sensitive to non-solenoidality
- FV methods can be used to benchmark other methods